Article:

eprints@whiterose.ac.uk
https://eprints.whiterose.ac.uk/

MDPI

Review

An Overview of Non-Isolated Hybrid Switched-Capacitor Step-Up DC–DC Converters

Julio C. Rosas-Caro [1,*], **Jonathan C. Mayo-Maldonado** [2,*], **Jesus E. Valdez-Resendiz** [3], **Avelina Alejo-Reyes** [1], **Francisco Beltran-Carbajal** [4] and **Oswaldo López-Santos** [5,6]

[1] Facultad de Ingenieria, Universidad Panamericana, Alvaro del Portillo 49, Zapopan 45010, Mexico
[2] Department of Electronic and Electrical Engineering, The University of Sheffield, Sheffield S102TN, UK
[3] Tecnologico de Monterrey, Av. Eugenio Garza Sada 2501, C.P. 64849, Monterrey 64700, Mexico
[4] Department of Energy, Universidad Autónoma Metropolitana, Unidad Azcapotzalco,
Mexico City 02200, Mexico
[5] Facultad de Ingeniería, Universidad de Ibagué, Carrera 69 Calle 22 Barrio Ambalá, Ibagué 730001, Colombia
[6] Departament d'Enginyeria Electrònica Elèctrica i Automàtica (ETSE), Universitat Rovira i Virgili,
43007 Tarragona, Spain
* Correspondence: crosas@up.edu.mx (J.C.R.-C.); j.mayo@sheffield.ac.uk (J.C.M.-M.);
Tel.: +52-33-1918-1065 (J.C.R.-C.); +44-78-9739-6363 (J.C.M.-M.)

Featured Application: Power conversion for electrical engineering and appliances.

Abstract: The increasing interest in renewable energy sources has brought attention to large voltage-gain dc–dc converters; among the different available solutions to perform a large voltage-gain conversion, this article presents an overview of non-isolated dc–dc converter topologies that utilize switched-capacitor circuits, i.e., diode-capacitors voltage multipliers. The review includes combinations of a traditional power stage with a diode-capacitor-based voltage multiplier, such as the multilevel boost converter. This article starts by reviewing switched-capacitor (SC) circuits, different topologies, and different types of charge exchange; it provides a straightforward analysis to understand the discharging losses. It then covers the multilevel boost converter and other topologies recently introduced to the state-of-the-art. Special attention is put on SC circuits with resonant charge interchange that have recently been probed to achieve very good efficiency. An additional contribution of the article is new proof of the discharging losses in resonant switched-capacitor circuits focused on the initial and final stored energy in capacitors, and this proof explains the relatively large efficiency obtained with SC resonant converters.

Keywords: multilevel boost converter; voltage multiplier; switched-capacitor converter

1. Introduction

Climate-change-related problems have focused the attention on renewable energy sources as an option to fossil fuels for electric energy generation [1–8]. Photovoltaic (PV) panels and fuel cells (FC) stacks are among the most studied renewable energy sources, but they produce electrical energy at a relatively low voltage; their voltage levels need to be boosted before being injected into the utility grid. This is one reason why much attention has been put on high-voltage gain dc–dc converters in the power electronics research field. Dc–dc converters usually perform the first energy conversion on PV generation systems to feed Voltage Source Converters (VSC) and integrate renewable energy into the utility grid [9–12].

Power electronics-based converters have been used extensively in this application [9–12]; several converters, such as the boost, buck-boost, Cuk, etc., can be used to increase the voltage to an adequate level. Traditionally, dc–dc converters are made by inductors, capacitors, and switches. Switches can be synthesized with diodes, transistors (such as

MOSFETS), or thyristors. Additionally, magnetic elements, such as coupled inductors or transformers, can be used [9].

The inductor is usually the largest and heaviest component in a power converter. An important research area related to the power electronics circuits is to achieve power conversion without inductors; in this case, Switched-Capacitor (SC) circuits are being investigated [13–116]. They are composed of capacitors and switches, and their research is not new, but their combination with traditional converters and/or with small inductors that produce a resonant charge interchange is giving a new breed to the research of SC converters [40–116], converters in which capacitors get charge interchange between them to increase or reduce the voltage.

This article presents an overview of hybrid SC converters. It starts with a short review of pure SC circuits [13–39], but it focuses on modifications of those circuits mainly with the use of small resonant inductors, which leads to resonant SC circuits [40–45,102–116], and the combination of traditional converters, such as the boost converter topology, with capacitor-based voltage multipliers [47–101].

It is important to emphasize that inductors used in resonant SC circuits are much smaller than energy storage inductors used in traditional converters. Their inductance is so small that some articles utilize air-core inductors or parasitic inductance in wires to achieve the resonant charge interchange [108,110–112]. The resonant charge interchange is a relatively new tendency among designers of SC circuits; it is relevant since several converters have been investigated with relatively large efficiency [40–45,102–116]. The efficiency of pure SC circuits is limited due to an effect in which the charge interchange among capacitors produces a type of loss which can be called discharging loss. It has been proved before that SC converters with a resonant charge interchange have no discharging losses, as will be discussed later.

The overview includes contributions introduced to the state-of-the-art in the last decade. Particularly converters under study are non-isolated and unidirectional in terms of power flow; most of them can be adapted to provide a bidirectional power flow, with the cost of increasing the number of transistors.

The two main types of SC circuits are pure SC circuits [13–39] and resonant SC circuits [40–45,102–116]. Resonant circuits utilize a small inductor to produce a resonant-type sinusoidal current, but only one half cycle is used to transfer charge among the capacitors before disconnecting them. A resonant design helps control the maximum or peak current among capacitors. References [13–16] have been dedicated to reviewing pure SC converters; this article extends the analysis to SC converters with resonant charge interchange [40–45,102–116] and hybrid converters, converters that contain one or more energy stored inductors [51–101].

In addition to the overview, which is the article's main contribution, an analysis is presented to explain the discharging losses, a difference between the initial and final amount of stored energy in the capacitors when connected in parallel. It is well known that when two capacitors are connected in parallel, the final stored energy (after the interconnection) is smaller than the initial stored energy. These types of energy losses are called discharging losses. The analysis presented in this article explains this phenomenon and how to ensure that discharging losses remain less than a particular percentage (for example, 5%). Furthermore, proof is provided to demonstrate that no losses are present due to the discharging phenomenon when the transferred energy is resonant (which can be achieved with a small resonant inductor). The provided proof is different from other proofs presented in the literature, i.e., [43], and it is based on the amperes per second and charge conservation principles; those bases are very well understood by power electronics engineers, which improves the knowledge of this phenomena.

2. Classification of Switched Capacitors Converters

As mentioned before, this manuscript is not dedicated to pure switched-capacitor circuits, but to their combination with traditional converters, their resonant versions, and

the combination of resonant SC circuits with traditional converters. However, a short overview of pure SC circuits is presented as an introduction. Then, the resonant charge interchange will also be introduced. Before going to topologies, the reader may look at [13–16] for a more exhaustive overview of the pure or classical SC circuits.

The main classification we can mention of SC circuits is shown in Figure 1, and is separated into two main types: *(i)* First, the circuits that do not need transistors are usually made of diodes and capacitors only, and these types of converters can be divided into, *(i.1)* ac-to-dc rectifiers with voltage multiplication characteristics, and the other type of SC converter that does not need transistors which is *(i.2)* circuits fed by digital signals used to produce a voltage larger than the digital input level.
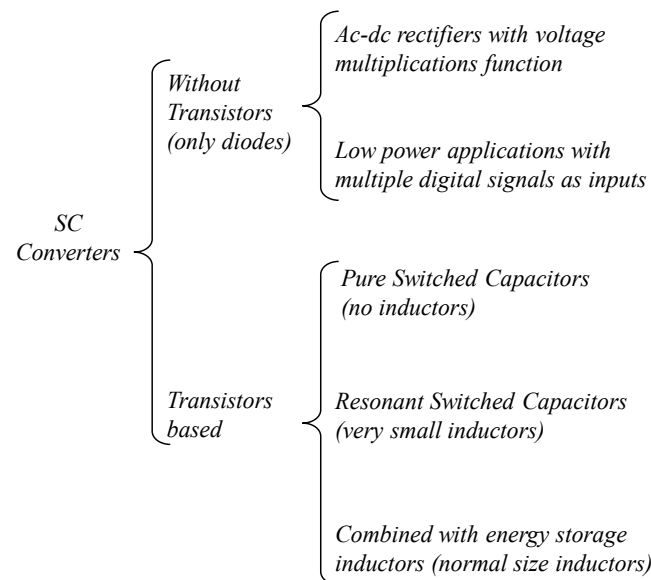
Figure 1. The main classification of SC converters.

SC circuits based on transistors can be divided into three main types, *(ii.1)* pure switched-capacitor circuits (circuits without inductors), *(ii.2)* SC converters with resonant charge interchange (circuits with tiny inductors), and finally, *(ii.3)* SC converters (either pure or resonant) combined with stored energy inductors (inductors in which linear ripple approximation can be applied to their current).

Let us start with a short overview of those different circuits.

2.1. Ac–Dc Rectifiers with Voltage Multiplication Function and a Single Input Signal

The first SC circuits were ac–dc converters whose driving signal was the ac input voltage, changing from positive to negative open and closing certain diodes. Figure 2a shows an ac-to-dc switched-capacitor voltage doubler. The input voltage is an ac voltage source, and it has a cycle in which it changes from positive to negative periodically. During their negative half cycle, a current flowed through the diode s_1 charging capacitor C_1 to the maximum voltage of the ac-source and, during this time, the circuit behaves in a similar way to the equivalent circuit shown in Figure 2b. In the other half cycle, when the input voltage is positive (see Figure 2c), the voltage from the source adds to the voltage in capacitor C_1, charging capacitor C_2 with twice the input voltage. This kind of converter was studied mainly at the beginning of the past century [13,14].

The circuit in Figure 2 can be extended in several ways. Some of the most common configurations are shown in Figure 3, where 6× rectifiers are shown, which means their output is six times their maximum input voltage. All of them have the voltage doubler as their core circuit, Figure 3a shows a topology in which series-connected capacitors make both sides of the converter, and the topology in Figure 3b shows a combination in which capacitors connected to the same point (that we can call grounded) made the left side of

the multiplier, while series-connected capacitors made the right side of the multiplier. The other two combinations can also be implemented, Figure 3c shows a combination in which series-connected capacitors made the left side of the multiplier while grounded capacitors made the right side, and finally, Figure 3d shows the topology with both sides (left and right) made by grounded-capacitors.
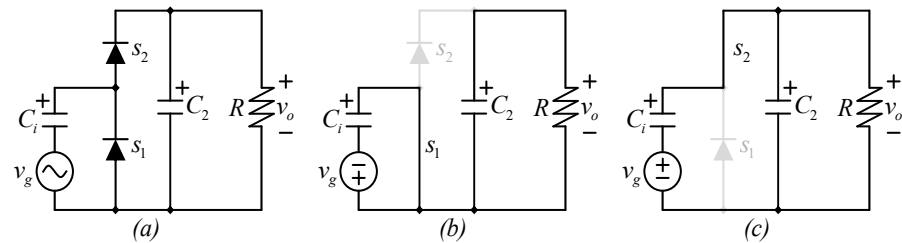
Figure 2. Ac-to-dc switched-capacitor voltage doubler (**a**) topology, (**b**) equivalent circuit when the input voltage is the negative half cycle, (**c**) equivalent circuit when the input voltage is in the positive half cycle.
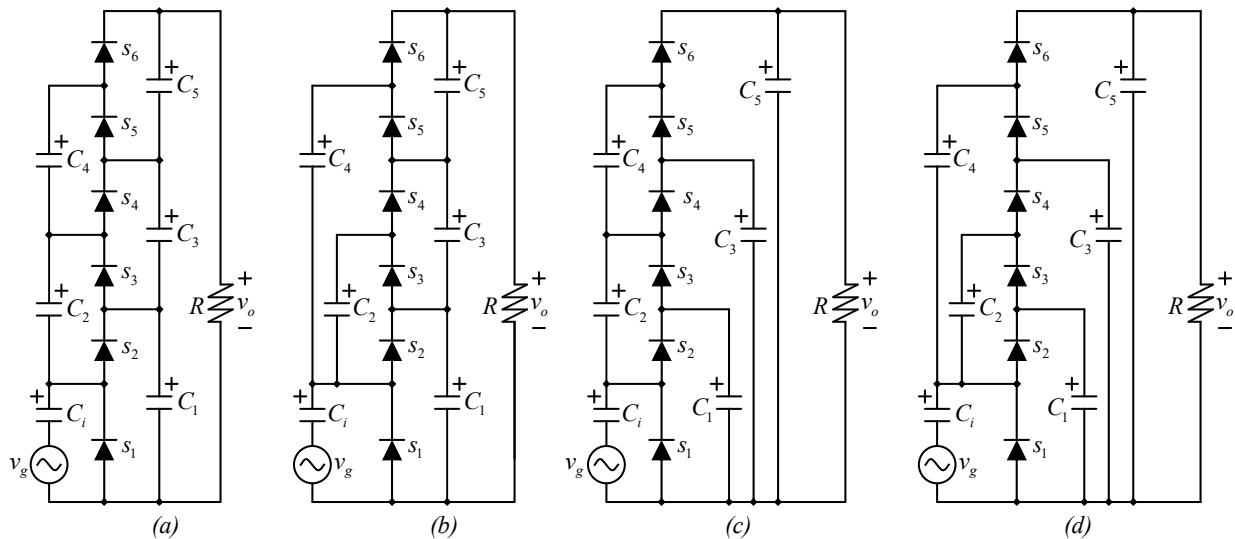
Figure 3. Several topologies of ac-to-dc switched-capacitor voltage multiplier ($\times 6$ multiplier) (**a**) both side series capacitor topology, (**b**) combination of grounded (**left**) and series (**right**) topology, (**c**) combination of series (**left**) and grounded (**right**) topology, and (**d**) both sides (**left** and **right**) grounded topology.

2.2. SC Voltage Multipliers with Digital Input Signals

The single-phase rectifiers mentioned in the last section were mainly used to obtain a large dc voltage from the utility grid, especially for generating a large electric field in particle accelerators. Still, their main applications were to obtain a relatively large voltage in electronic circuits, for example, digital circuits [17,18]. An example of these multiple inputs, which are usually digital signals, is shown in Figure 4 (as shown in [18]).
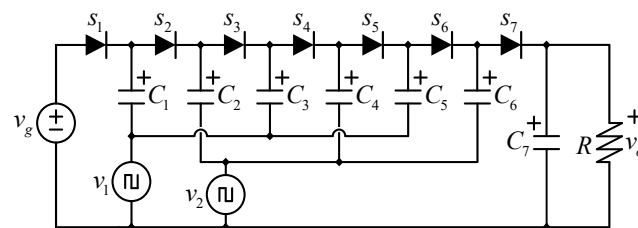
Figure 4. A multiple auxiliary input SC voltage multiplier [18].

The input voltage in Figure 4 is a dc signal; the converter does not contain transistors, but two additional input pulsating signals drive the converter. Those additional pulsating signals are digital, and they take values of high and low that can, instead, be 5 V for high and 0 V for low. They are square signals with a phase shift of 180° between them; this produces only two equivalent circuits because when one signal is high, the other is low. The additional input signals are called v_1 and v_2. Figure 5 shows the two equivalent circuits.
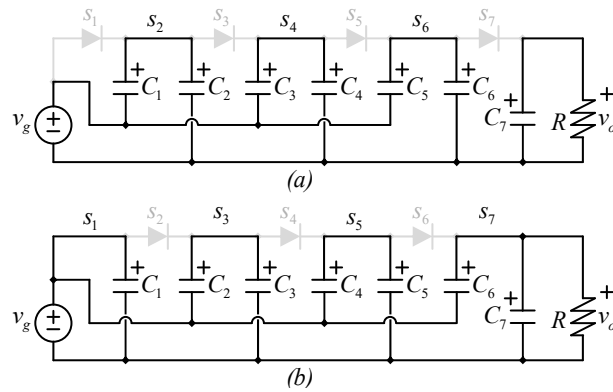
Figure 5. Equivalent circuits of the multiplier in Figure 4. (**a**) First equivalent circuit when v_1 is high and v_2 is low, and (**b**) second equivalent circuit when v_2 is high and v_1 is low.

Input signals v_1 and v_2 in Figure 5 act as one firing signal with their complement, v_1, being a square signal (50% of duty cycle), and v_2 being their complementary signal; v_2 is high when v_1 is low and vice versa. This produces two equivalent circuits shown in Figure 5.

In Figure 5b, capacitor C_1 is charged with the input voltage v_g, at the second semi-cycle (Figure 5a). The capacitor C_1, in series with the input voltage source, charges C_2 with twice the input voltage in the next semi-cycle (Figure 5b), the capacitor C_2, in series with the input voltage source, charges C_3 with three times the input voltage. In the next semi-cycle (Figure 5a), the capacitor C_3, in series with the input voltage source, charges C_4 with four times the input voltage, and so on. The circuit in Figure 5 produces an output equal to seven times the input voltage.

Other topologies can work with the same principle; for example, Figure 6 shows a simplification of the circuit in Figure 4, in which one of the digital signals is always low, and only one digital signal is required, but in this case, the voltage gain is smaller than in Figure 4.
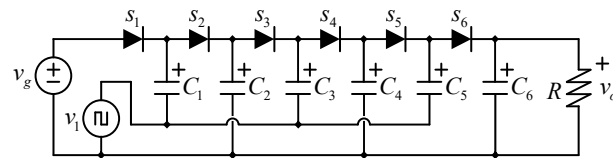
Figure 6. A reduced version of the converter shown in Figure 4 [18].

There are other topologies with multiple digital (or AC) inputs and a dc power source, and a voltage multiplier can be fed only with digital signals (without the dc source); as an example, see Figure 7, as shown in [17].

Figure 7. A multiple auxiliary input SC voltage multiplier.

2.3. SC Controlled by Transistors, the Elementary Principle

One realization of a voltage doubler similar to the digital-signals-driven SC converters can be seen in Figure 8. Instead of using a digital signal as in Figure 6, two transistors generate the pulses for capacitor C_1. Figure 8a shows the more basic circuit with an auxiliary pulsating signal. Figure 8b shows how the pulsating signal can be produced with two transistors that connect the low side of capacitor C_1 either to the positive or to the negative side of the input voltage source.

(a) Transistor-less SC voltage doubler
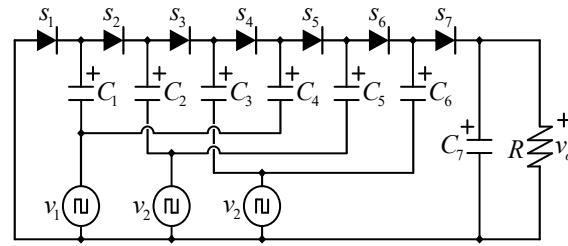
(b) Transistors based SC voltage doubler
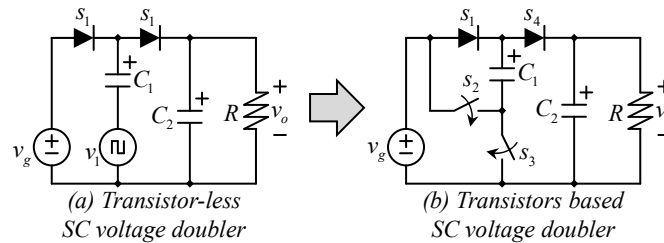
Figure 8. Switched-capacitor voltage doubler, the simplest configuration of the converter in Figure 6, (**a**) with an auxiliary pulsating signal and (**b**) based on two transistors and two diodes.

Diodes and transistors are basically switches. Figure 9 shows the same topology with switches in all semiconductors, this does not modify the original idea, and sometimes in dc–dc conversion, switches are used instead of diodes since they have lower conduction losses. Figure 8 shows what we can consider as the conversion from the digital signals-driven SC circuits to the modern SC circuits based on the transistors.

(a) SC voltage doubler

(b) $s_1=s_3=1$, $s_2=s_4=0$.

(c) $s_1=s_3=0$, $s_2=s_4=1$.
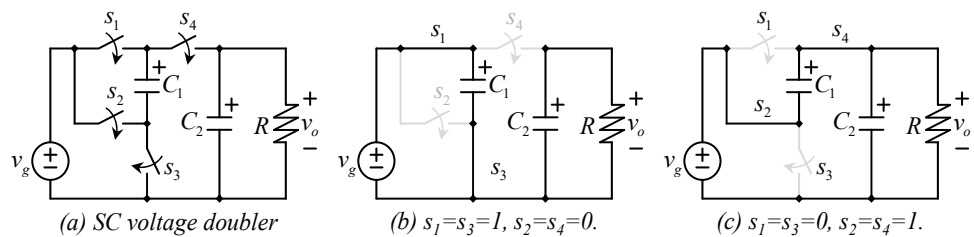
Figure 9. Switched-capacitor voltage doubler, (**a**) four switches-based topology, (**b**) equivalent circuit when switches s_1 and s_2 are on while s_2 and s_4 are off, (**c**) equivalent circuit when switches s_1 and s_2 are off while s_2 and s_4 are on.

Let us consider the circuit in Figure 9a, which can be classified as a pure SC voltage doubler. The circuit in Figure 9a is equivalent to the one shown in Figure 8b, but it has only switches or transistors, four transistors instead of two diodes and two transistors. Switches s_1 and s_3 are driven with the same switching signal, a square signal (50% of duty cycle), and switches s_2 and s_4 are also driven with the same firing signal, which is the complementary function to the first one. Two equivalent circuits are produced in this operation, as shown in Figure 9b,c.

Figure 9b shows the switching state or equivalent circuit of the converter when s_1 and s_3 are on ($s_1 = s_2 = 1$) while s_2 and s_4 are off ($s_2 = s_4 = 0$). Figure 9c shows the other switching state when s_1 and s_3 are off ($s_1 = s_2 = 0$) while s_2 and s_4 are on ($s_2 = s_4 = 1$).

When the circuit is in the state shown in Figure 9b, capacitor C_1 gets charged to the input voltage, and in the other state (see Figure 9c), C_1 gets in series with the input voltage source charging C_2 with twice the input voltage. The load resistance discharges the capacitor C_2, but if the capacitance value of the capacitors and the switching frequency are large enough, it is possible to design a circuit with a relatively small output voltage ripple.

The parallel interconnection of the capacitors is the main difference between the operation of switched-capacitor circuits and traditional converters (such as the buck or boost); switched-capacitor circuits are intended to avoid inductors for which the energy interchange must be done with the unique energy stored components on the circuits, the "Capacitors".

The circuit shown in Figure 9 is only a member of a larger family in which many combinations can be configured and extended. Pure SC topologies have been studied since the 1970s when the most traditional topologies were introduced. They were used as voltage multipliers to produce a larger voltage than their input. The first classification we may introduce to pure switched-capacitor circuits is that there are SC circuits in which input signals drive the switches, for example, in AC–DC voltage multipliers, and converters in which switches drive the operation.

3. Switched-Capacitor Circuits Controlled by Transistors

We studied several SC topologies with transistors and have described the most common. For example, Figure 10a shows a possible circuit extension in Figure 9. It can be called the *Series-Parallel Converter*, one of the converters studied in [20].
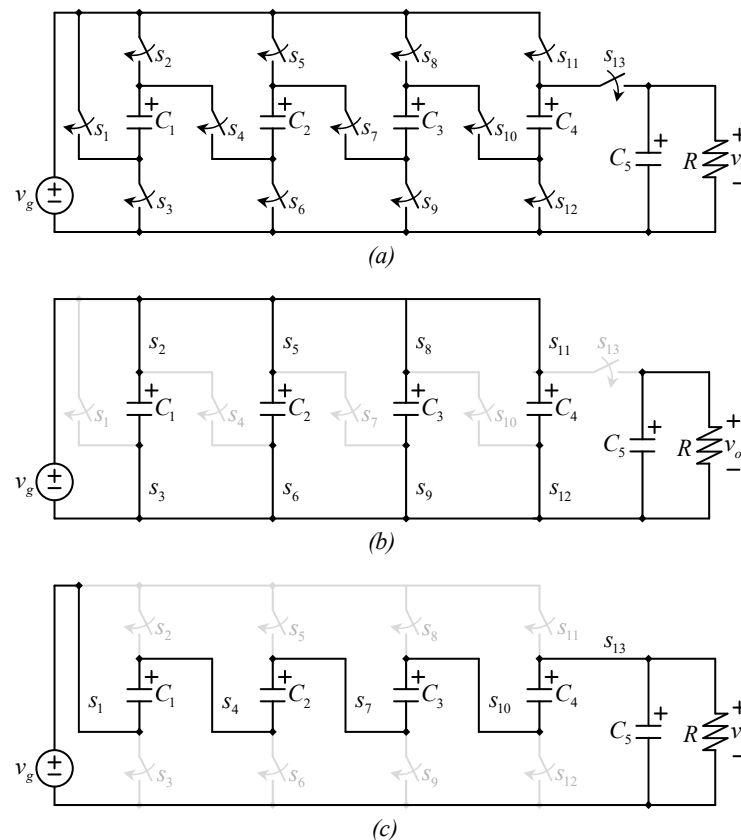
Figure 10. The *Series-Parallel Converter* and their equivalent switching states, (**a**) topology, (**b**) equivalent circuit when capacitors are in parallel, and (**c**) equivalent circuit when capacitors are in series.

Figure 10 also shows the equivalent circuits in the two switching states of the converter. As their name indicates, one of the switching states (see Figure 10b) corresponds to a state in which all capacitors (except the output capacitor) are in parallel, while Figure 10c shows an

equivalent circuit when all capacitors (except the output capacitor) are in a series connection. This operation can be summarized as follows from Figure 10a: We can divide the switches into two groups; group *A* is made by switches s_2, s_3, s_5, s_6, s_8, s_9, s_{11}, and s_{12}, and group *B* is made by s_1, s_4, s_7, s_{10}, and s_{13}. We drive the converter with a single firing signal, a square signal (50% of duty cycle), meaning the switches of group *A* are all closed, and the switches of group *B* are all open when the firing signal is one (high). This produces the equivalent circuit shown in Figure 10b. On the other hand, when the firing signal is zero (low), the switches of group *A* are all open while the switches of group *B* are all closed; this produces the equivalent circuit shown in Figure 10c.

When the circuit behaves in the same way as in Figure 10b, capacitors C_1, C_2, C_3, and C_4 get connected in parallel to the input voltage and charged to the input voltage level. In the other state, those capacitors (C_1, C_2, C_3, and C_4) get in series with the input voltage source charging C_5 with five times the input voltage.

This converter, which is the *Series-Parallel Converter*, multiplies the input voltage for a certain value. In the case of Figure 10, the input voltage is multiplied by five, and this value can be extended with more capacitors and switches.

The *Series-Parallel Converter* is one of the possible extensions to the circuit in Figure 9. Another possible extension is shown in Figure 11; it is known as the *Fibonacci Converter* [21] (another of the converters studied in [20]).
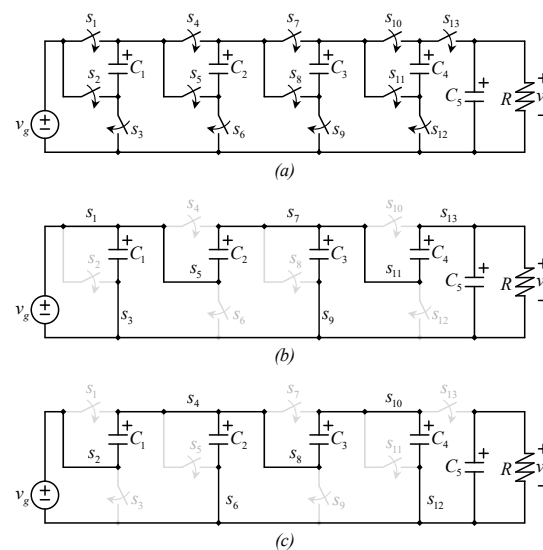
Figure 11. The *Fibonacci Converter* is another possible extension to the circuit in Figure 9, (**a**) topology, (**b**) equivalent circuit when the single firing signal is high, and (**c**) equivalent circuit when the single firing signal is low.

Figure 11 also shows the equivalent circuits of the Fibonacci Converter. The converter may seem to be operated with two firing signals, square signals with a phase shift of 180°, or with a single firing signal in which some of the transistors are driven on when the firing signal is high, while other transistors are driven on when the firing signal is low.

Their traditional operation can be described in the following manner. Again, we can divide the switches into two groups: group *A* is made by odd switches (s_1, s_3, s_5, s_7, s_9, s_{11}, and s_{13}), and group *B* is made by even switches (s_2, s_4, s_6, s_8, s_{10}, and s_{12}). We can also drive the converter with a single firing signal, a square signal (50% of duty cycle), meaning the switches of group *A* are all closed, and the switches of group *B* are all open when the firing signal is one (high), which produces the equivalent circuit shown in Figure 11b. On the other hand, when the firing signal is zero (low), the switches of group *A* are all open, while the switches of group *B* are all closed; this produces the equivalent circuit in Figure 11c.

When the circuit behaves as in Figure 11b, capacitor C_1 gets charged with the input voltage at the next switching state (see Figure 11c). C_1, in series with the input voltage,

charges C_2 with twice the input voltage at the next switching state when the circuit behaves again as Figure 11b, with C_1 in series with C_2, which charges C_3 to three times the input voltage. Then, back in Figure 11c, C_2, in series with C_3, charges C_4 with five times the input voltage. Finally, back in Figure 11b, C_3, in series with C_4, charges capacitor C_5 with eight times the input voltage.

The circuit is called the *Fibonacci Converter* since capacitors get charged with multiples of the input voltage, and the multiples are equal to the Fibonacci series of numbers (considering the input voltage as the first one), which is 1, 1, 2, 3, 5, 8 ... , (the following number is the sum of two previous numbers).

The circuit in Figure 11 can acquire gains which are different to the Fibonacci series; for example, if group A is made by the switches s_1, s_3, s_4, s_6, s_7, s_9, s_{10}, and s_{12}, and group B is made by all the other switches (s_2, s_5, s_8, s_{11}, and s_{13}), their switching states would be equivalent to Figure 10b,c, and the gain would be linear. As with the *Series-Parallel*, other switching sequences can be tried.

One of the last classical SC converters covered is the *Ladder Converter*, see Figure 12a. This converter cannot be considered as an extension of the converter in Figure 9, at least not in a straightforward manner, and this is one of the most popular SC circuits nowadays [22–26].
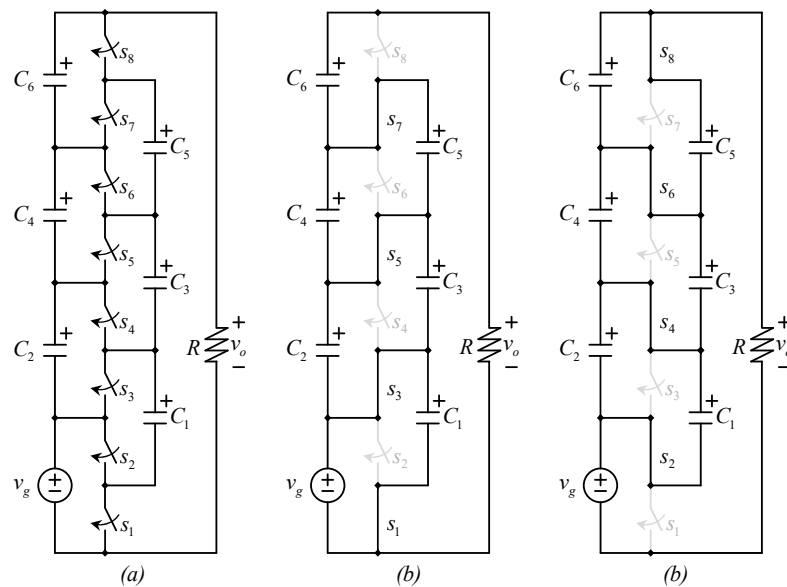
Figure 12. The *Ladder Converter* is another possible extension to the circuit in Figure 9. (**a**) Converter topology, (**b**) equivalent circuit when the firing signal is high, and (**c**) equivalent circuit when the firing signal is low.

Following the same procedure used to discuss the operation of the *Series-Parallel* and *Fibonacci* converters, we can divide the switches into two groups: group A, made by all the odd switches, and group B, made by all the even switches. By driving the converter with a single firing signal, a square signal (50% of duty cycle), the switches of group A are all closed, and the switches of group B are all open when the firing signal is one (high), which produces the equivalent circuit shown in Figure 12b. On the other hand, when the firing signal is zero (low), switches of group A are all open while switches of group B are all closed; this produces the equivalent circuit shown in Figure 12c.

The parallel connection between capacitors means that all capacitors are charged to the input voltage, the converter can be extended with more switches and capacitors, and the circuit's output voltage in Figure 12 is four times the input voltage.

This converter can be considered the transistorized version of a *Cockcroft–Walton Voltage Multiplier* or *Ladder Voltage Multiplier*, a rectifier or ac-to-dc converter that utilizes the alternating voltage to activate diodes. Several studies have been done with this converter, such as [22–26].

The resonant version of this converter has been used in several applications, mainly in voltage equalizers for either batteries or capacitors connected in series, as mentioned in Section 5.4.

Converters in this section are presented in the form of their step-up topology, but, in all cases, they can also work as a step-down converter by inverting their source and load side.

The field of investigating new topologies is very active among the recent contributions to the state-of-the-art in topologies of the SC circuits. One of the recently investigated topologies is the *Flying Capacitor Multilevel Inverter* [27–31], see Figure 13. Initially used as a multilevel inverter, it has also been investigated as a dc–dc SC converter.
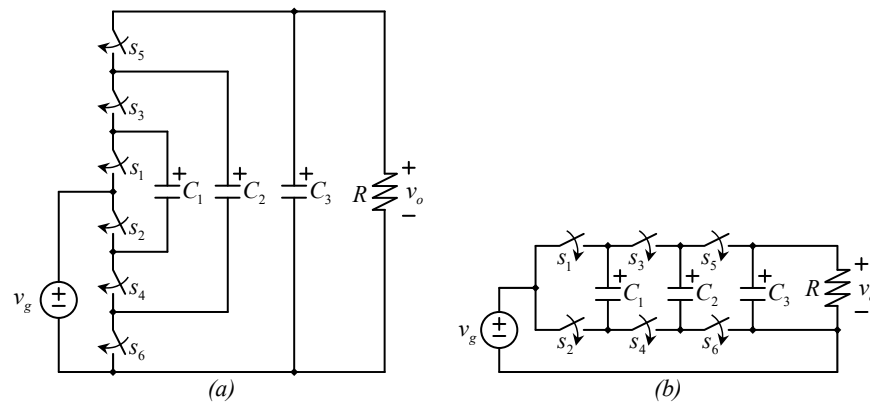
Figure 13. Two common ways of drawing the Flying Capacitor Multilevel Converter (it is the same topology drawn in two different ways), (**a**) drawn in vertical way, (**b**) drawn horizontally.

Figure 13 shows the converter used as a $3\times$ converter, which means the output voltage (or high-side voltage) is three times the input voltage (or high-side voltage). To perform this conversion, three switching states are required instead of two, as in the previously studied converters. Figure 14 shows the switching states of the converter in Figure 13.
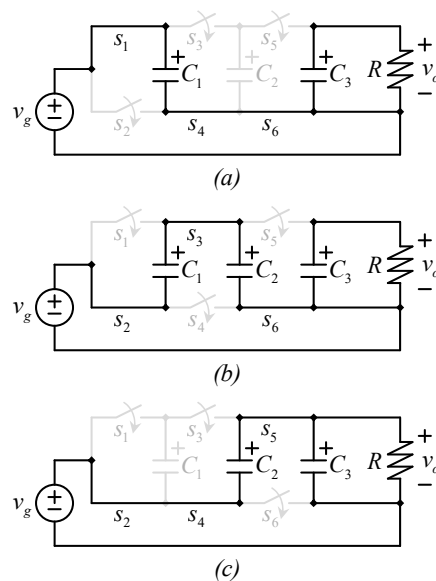
Figure 14. The three states of the switching sequence of the converter shown in Figure 13, (**a**) first switching state, (**b**) second switching state, and (**c**) third switching state.

The *Flying Capacitor Converter* was not proposed as an SC circuit, but as a dc–ac (or ac–dc) converter, but it can also be used as an SC dc–dc converter, although it requires more sophisticated switching functions.

The converter in Figure 13 requires three equivalent circuits to operate. Figure 14 shows those equivalent circuits, and Figure 14a shows the equivalent circuit in which switches s_1, s_4, and s_6 are on while s_2, s_3, and s_5 are off. We call this the first switching state. Figure 14b shows the equivalent circuit in which switches s_2, s_3, and s_6 are on while s_1, s_4, and s_5 are off. We call this the second switching state. Figure 14c shows the equivalent circuit in which switches s_2, s_4, and s_5 are on while s_1, s_3, and s_6 are off. We call this the third switching state.

As a short discussion of advantages and disadvantages, the *Fibonacci Converter* has a voltage gain that increases significantly when the number of power stages increases, in contrast to the *Ladder* and the *Series-Parallel,* whose voltage gains increase linearly when the number of power stages increases. The *Ladder* and the *Series-Parallel* have the advantage of having the same voltage in all capacitors, equal to the input voltage. The *Ladder* has the advantage against the other two in that switches are also rated to the input voltage. The *Series-Parallel* and the *Fibonacci* require transistors of a larger voltage as the number of power stages increases. The *Flying Capacitor* topology has the same voltage in all switches, but a different voltage across capacitors. It requires three switching states instead of two.

One of the most recent contributions to the SC topologies was the proposition of the *Multilevel Modular Capacitor-Clamped DC–DC Converter* or the MMCC Converter [32]. Figure 15 shows the MMCC Converter.
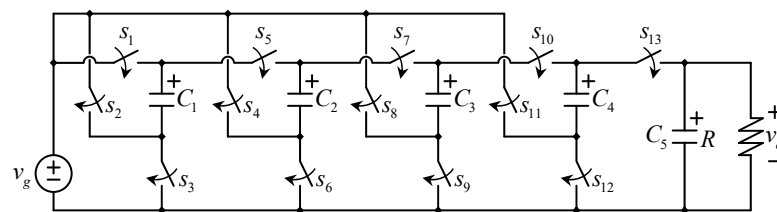
Figure 15. The MMCC Converter topology.

The operation can be explained in the following manner: The digital inputs are divided into two groups with the same firing signal; similar to the former SC converters, it has two equivalent circuits (except for the flying capacitor, which has three).

Figure 16a shows the first equivalent circuit; in this state, switches s_1, s_3, s_4, s_7, s_9, s_{11}, and s_{13} are on, while s_2, s_5, s_6, s_8, s_{10}, and s_{12} are off. Figure 16b shows the second equivalent circuit; in this state, switches s_1, s_3, s_4, s_7, s_9, s_{11}, and s_{13} are off, while s_2, s_5, s_6, s_8, s_{10}, and s_{12} are on.

(a)

(b)
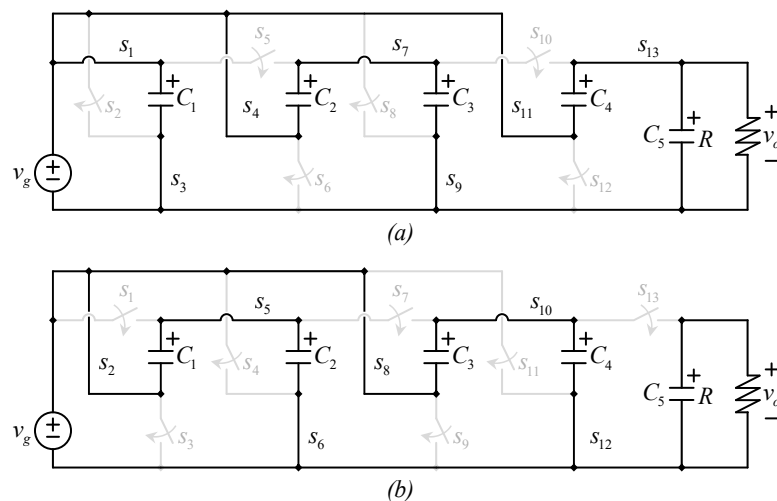
Figure 16. Equivalent circuits of the *MMCC Converter*, (**a**) first switching state, (**b**) second switching state.

During the first switching state, capacitor C_1 gets charged to the input voltage v_g. During the second state, C_1, in series with the input voltage, charges C_2 to twice the input voltage. Then, in the following switching state (back to the first state), C_2, in series with the input voltage, charges C_3 with three times the input voltage. In the next state, C_3, in series with the input voltage, charges C_4 with four times the input voltage. Finally, C_4, in series with the input voltage, charges C_5 with five times the input voltage. The topology can be extended. In the case of Figures 15 and 16, we are depicting an 5× voltage multiplier.

By analyzing the equivalent circuits or switching states, the MMCC converter work in some way as a transistors-based version of the converter in Figure 4, but each capacitor has a pair of transistors that work as its "digital" inputs (instead of separate pulsating signals).

Following the comparison and discussion, the MMCC converter seems similar to a combination of the *Series-Parallel* with the *Fibonacci*; it has the Fibonacci voltage gain, which means its voltage gain can be relatively large with few power stages. All capacitors and all switches have the same voltage stress equal to the input (or low side) voltage. Those advantages make it superior to previous topologies, which is why their development can be considered a significant contribution. Several articles have been dedicated to this converter, including their resonant charge interchange, as will be discussed in Section 5.4.

Table 1 shows a comparison of the transistors-based pure switched capacitors based on the number of switches, the maximum voltage stress on switches, the number of capacitors, the maximum voltage on capacitors, and the output voltage that can be used to obtain a voltage gain.

Table 1. Comparison between transistorized pure switched-capacitor converters.

Topology	Number of Switches	Maximum Voltage on a Switch	Number of Capacitors	Maximum Voltage on a Capacitor	Output Voltage
5× *Series-Parallel* (Figure 10a)	13	$4 \times V_g$	5	$5 \times V_g$	$5 \times V_g$
8× *Fibonacci* (Figure 11a)	13	$5 \times V_g$	5	$8 \times V_g$	$8 \times V_g$
4× *Ladder* (Figure 12a)	8	V_g	6	V_g	$4 \times V_g$
6× *Ladder* (no draw)	12	V_g	10	V_g	$6 \times V_g$
3× *Flying Capacitor* (Figure 13a)	6	V_g	3	$3 \times V_g$	$3 \times V_g$
5× *Flying Capacitor* (no draw)	10	V_g	5	$5 \times V_g$	$5 \times V_g$
5× *MMCC* (Figure 15)	13	V_g	5	$5 \times V_g$	$5 \times V_g$

4. The Charge Interchange between Capacitors

As mentioned before, one of the motivations for studying SC converters is the recent development of topologies with a relatively high efficiency at a relatively large power. For example, [104] reported an efficiency of 99% with a 22 kW prototype. Table 2 shows some of the references in which switched converters are reported to have achieved a high efficiency. It can be observed that in those cases (mentioned in Table 2), the converters operate with a resonant charge interchange. This section discusses the different types of charge interchange among SC circuits and the analysis of stored energy (before and after the paralleling of capacitors).

**Table 2.** References of switched-capacitor converters with high efficiency.

Title	Reference	Peak Efficiency Reported	Power Rating of Experiment
Multilevel DC–DC Power Conversion System with Multiple DC Sources	[102]	98.9%	10 kW
Analysis and Comparison of Medium-Voltage High-Power DC/DC Converters for Offshore Wind Energy Systems	[104]	99.1%	22 kW
SiC-Based Bidirectional Multilevel High-Voltage Gain Switched-Capacitor Resonant Converter with Improved Efficiency	[105]	97%	5 kW
DC–DC High-Voltage-Gain Converters with Low Count of Switches and Common Ground	[107]	91%	300 W
Design and Analysis of Switched-Capacitor-Based Step-Up Resonant Converters	[109]	94.4%	100 W
Multiphase Multilevel Modular DC–DC Converter for High-Current High-Gain TEG Application	[110]	97%	650 W
Zero-Current-Switching Multilevel Modular Switched-Capacitor DC–DC Converter	[111]	98%	150 W
Switched-Capacitor-Cell-Based Voltage Multipliers and DC–AC Inverters	[112]	96%	1 kW
Resonant switched-capacitor voltage multiplier with interleaving capability	[113]	95.5%	150 W
LLC Resonant Voltage Multiplier-Based Differential Power Processing Converter Using Voltage Divider with Reduced Voltage Stress for Series-Connected Photovoltaic Panels under Partial Shading	[114]	99.6%	1.2 kW
Nonisolated High Step-Up Soft-Switching DC–DC Converter with Interleaving and Dickson Switched-Capacitor Techniques	[115]	97.9%	1 kW
Input Current Ripple Reduction in a Step-Up DC–DC Switched-Capacitor Switched-Inductor Converter	[116]	95%	700 W

It has been observed that traditional SC circuits have *discharging losses*. This section explains this term. It has also been observed and demonstrated that SC circuits with a resonant charge interchange seem not to have *discharging losses*. One of the contributions of this article is to provide a new demonstration (other demonstrations have been published before) based on the amperes per second and charge conservation principle. These principles are widely used and known for power electronics engineering, for which we think the analysis will be better understood.

4.1. Different Types of Charge Interchange

Switched-capacitor circuits have different applications; when they are used for power conversion, there is a disadvantage from the power electronics point of view; when capacitors get connected in parallel, the current among the capacitors, what we usually call the "charge interchange" [34,40,41], is limited only by parasitic resistances in both transistors and capacitors. This produces a spike-type waveform such as the ones shown in Figure 17. The circuit in Figure 17 shows two capacitors. Let us consider that they have different voltages before being paralleled ($V_{C1} > V_{C2}$). The resistor R_{Par} lumps the parasitic resistances of the loop, including both capacitors of ESR and the switch-on resistance. The peak current is equal to the initial voltage difference divided over the parasitic resistance R_{Par}. The current follows the classical exponential discharge. This does not make their applications

prohibited, there are many applications in power electronics for switched-capacitor circuits, and the peak current can be calculated and handled.
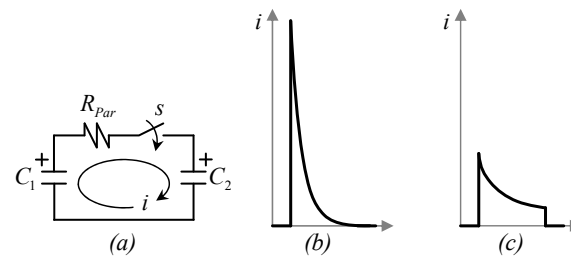
Figure 17. Basic non-resonant SC circuit, (**a**) schematic, (**b**) current between capacitors with full charge interchange, (**c**) current between capacitors with a partial charge interchange.

Despite the fact that the current waveform among the capacitors does not prohibit the application of SC circuits in power conversion, it presents the following concerns and disadvantages for high-power applications:

- If the peak current is too large, it may damage the components (transistors and capacitors). In transistors, a large current, such as the peak current in the SC converters, causes an increase in the switching losses of the transistor, increasing its junction temperature [117].
- A spike current has a larger RMS value than a flat one. It is better to have a flat current.
- There is an effort to reduce parasitic resistances in new devices, transistors, and capacitors; we can expect that the peak current will be larger if we use better components.

The peak of the current can be reduced if the switching frequency is high enough to prevent a large discharge of the output capacitor, leading to what we call "partial charge interchange" (see Figure 17), but this still is more used in low power since the switching losses of transistors may be larger.

Those concerns have limited the applications of what we now call "pure switched capacitors" circuits to low-power applications, but it has motivated the creation of another type of switched-capacitor circuits, which we call Resonant Switched Capacitors (RSC).

Resonant Switched-Capacitor (RSC) circuits contain small inductors to avoid a spike current while making those currents sinusoidal. It is important to emphasize that avoiding inductors was the motivation to develop SC converters, and then the inclusion of inductors may sound contradictory, but inductors used in RSC converters are pretty small compared to energy storage inductors used in traditional converters. Figure 18 shows a comparison of two inductors used in traditional converters (such as the boost converter) and a small inductor (0.2 μH) used in an RSC converter. Some articles have reported air-core inductors or the use of the parasitic inductance on wires to produce the resonant charge interchange [42].
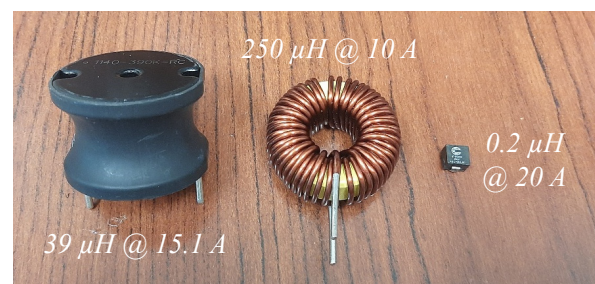
Figure 18. Comparison between two energy storage inductors and a tiny resonant inductor.

Figure 19 shows an equivalent circuit of two capacitors connected in parallel through a small resonant inductor, L_{res}; the current between the capacitors tends to be sinusoidal. We assume the switch opens when the current crosses zero to prevent the current from becoming negative.
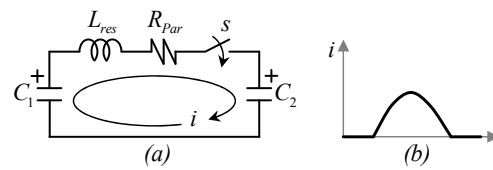
Figure 19. Basic resonant SC circuit, (**a**) schematic, (**b**) current between capacitors with resonant charge interchange.

The shape depends on the damping factor, as explained in [42], but as we can choose the capacitance and the inductance (and try to minimize the parasitic resistance), the designer can ensure the current is similar to a sinusoidal.

The resonant switching limits the peak current between capacitors; it produces a zero current switching and leads to better circuit efficiency. Conversely, the resonant period must be considered to avoid opening the resonant circuit before the current reaches zero. The main difficulty with the resonant-switched capacitor operation is that the current does not stop automatically when it reaches zero. It tends to produce a sinusoidal signal, typical in resonant circuits. It is important to open the switch exactly when the current reaches zero, which is difficult considering the resonant frequency may change due to the tolerance of components from one converter to another one. Another option is to use a diode to prevent the current from becoming negative [40,41].

The efficiency improvement on resonant switched-capacitor circuits compared to pure switched capacitors can be explained by analyzing the efficiency from the stored energy point of view [43]. The efficiency of a power converter is usually analyzed from the power consumption point of view, but the current shape (which depends on parasitic components) is not easy to determine on switched-capacitor circuits; the other option is the energy-based analysis.

4.2. Energy Analysis on the Non-Resonant Charge Interchange

The energy analysis is well known in the case of a pure switched-capacitor circuit; 50% of the data is in the mind of many researchers, but that 50% applies only in the case of a full-charge interchange of capacitors of the same capacitance, and when one of those capacitors is initially discharged. Let us start from the beginning to understand that value and analyze different cases.

Let us consider a circuit made only by two capacitors, C_1 and C_2, as in Figure 20. The capacitances of the capacitors and their initial voltage may be different. In addition, let us recall the well-known analogy between the studied system and a hydraulic system consisting of two interconnected water tanks since capacitors have the same mathematical model as water tanks.
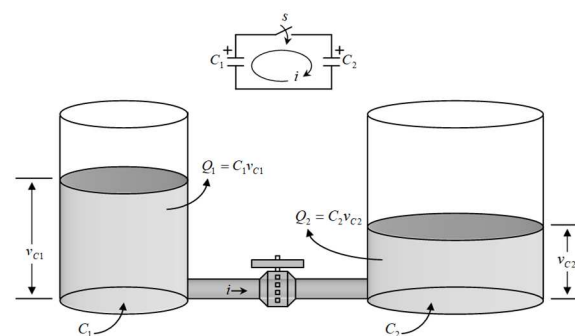
Figure 20. Pure switched-capacitors circuit and their hydraulic analogy.

For the energy-based analysis, it is not necessary to model parasitic resistances, which makes the analysis relatively simple. Let us consider whether capacitors get connected in parallel or whether we open the valve which connects the water tanks.

Capacitors are initially disconnected and have different initial voltages v_{1i} and v_{2i}, respectively. If the switch closes and remains closed until the current becomes zero, a full charge interchange process will take place. The current would be similar to the one shown in Figure 17, leading to a new equilibrium; this process may be, ideally, instantaneous (in the ideal case of zero parasitic resistance), and some charge will be transferred from the capacitor with a larger initial voltage to the capacitor with a smaller initial voltage. After the transient, both capacitors will be charged to the same final voltage v_f.

From the charge conservation principle, the initial and final charge of the circuit must be the same, which can be expressed as:

$$C_1 v_{1i} + C_2 v_{2i} = C_1 v_f + C_2 v_f = (C_1 + C_2) v_f \tag{1}$$

From the circuit (or the water tanks analogy), the final voltage v_f can be expressed as in Equation (2).

$$v_f = \frac{C_1 v_{1i} + C_2 v_{2i}}{C_1 + C_2} \tag{2}$$

Let us focus on the stored energy in both the initial and final states. The initial stored energy can be expressed as (3),

$$\varepsilon_0 = \frac{C_1 v_{1i}{}^2}{2} + \frac{C_2 v_{2i}{}^2}{2} \tag{3}$$

while the stored energy at the final state, after the transient, can be expressed as in Equation (4).

$$\varepsilon_f = \frac{C_1 V_f^2}{2} + \frac{C_2 V_f^2}{2} = \frac{(C_1 + C_2) V_f^2}{2} \tag{4}$$

By substituting (2) into (4), the stored energy after the transient can be expressed as in Equation (5):

$$\varepsilon_f = \frac{(C_1 + C_2)}{2} \left(\frac{C_1 v_{1i} + C_2 v_{2i}}{C_1 + C_2} \right)^2 = \frac{(C_1 v_{1i} + C_2 v_{2i})^2}{2(C_1 + C_2)} \tag{5}$$

The difference between the initial and final stored energy depends on the parameters and initial conditions of the system. Let us consider the case in which both capacitors have the same capacitance ($C_1 = C_2 = C$ in (5)). The final stored energy would be expressed as (6).

$$\varepsilon_f = \frac{C}{4} (v_{1i} + v_{2i})^2 \tag{6}$$

Now, let us define a ratio of the final over the initial energy "η_ε" by dividing (6) over (3); this can be a measure of efficiency by considering that the initial state contains the input energy and the final state contains the output energy, and it can be expressed as

$$\eta_\varepsilon = \frac{\frac{C(v_{1i} + v_{2i})^2}{4}}{\frac{C(v_{1i}{}^2 + v_{2i}{}^2)}{2}} = \frac{(v_{1i} + v_{2i})^2}{2(v_{1i}{}^2 + v_{2i}{}^2)} = \frac{1}{2} + \frac{v_{1i} v_{2i}}{v_{1i}{}^2 + v_{2i}{}^2} \tag{7}$$

Figure 21 shows a graph of (7) as a function of the ratio among v_{2i} divided over v_{1i}. We are considering that the voltage in C_1 is initially larger, but the same case would be obtained in the other case with an inverse flow of the current and power.
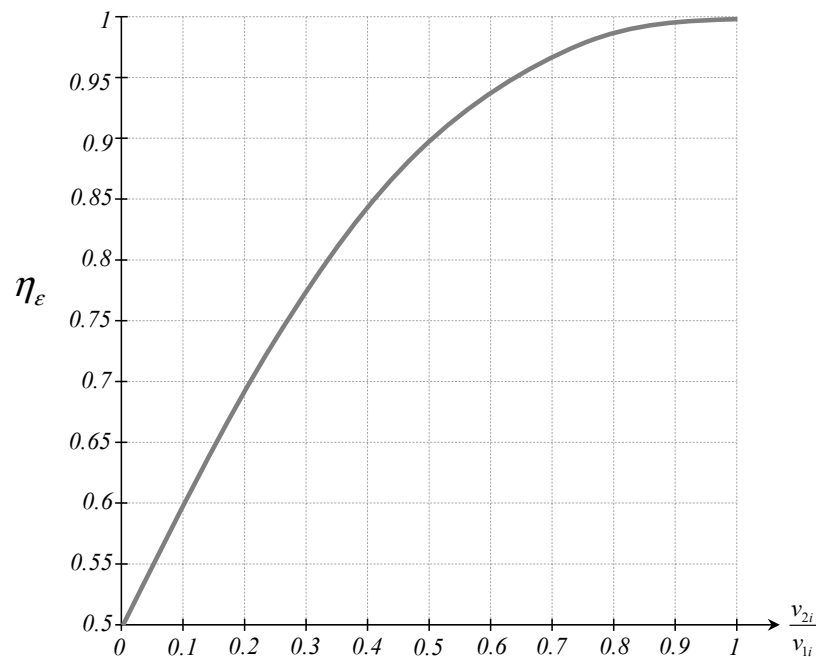
Figure 21. Store energy ratio among the final and the initial condition.

There are many things we can discuss in this experiment; some important comments are:

(i) The stored energy ratio is always smaller than 1, which is expected from the efficiency analysis in the power converters.

(ii) The capacitance of the capacitors seems to disappear from (7), but this is only when the capacitors are equal. If the capacitors are different, the ratio among the capacitances would appear as a factor in Equation (7).

(iii) The minimum ratio (or efficiency) observed when capacitors are equal is 0.5 of 50%, but this is only the minimum. The efficiency may be larger if the second capacitor initially has more than 50% of the other one. The efficiency remains over 90%. On the other hand, if one capacitor's initial voltage is smaller than 50% of the other, the efficiency decreases rapidly.

(iv) The efficiency is larger if the initial difference of the voltages is smaller, but if the initial voltage of the capacitors is equal, the charge interchange would be zero. Then, the 100% efficiency has a trade-off versus the amount of charge transferred. This is another way of seeing why pure SC circuits are mainly used in low-power applications.

We can say the ratio between the final over the initial stored energy has an impact on the efficiency based on the principle of connecting capacitors in parallel.

Another interesting commend is that the power losses found in this analysis do not depend on the parasitic resistance that connects capacitors, but a low parasitic resistance would lead to a faster charge interchange (which is an advantage) and a larger peak current (which is a disadvantage).

This kind of analysis is not common in other types of converters, in which losses are analyzed from the power dissipation point of view.

Before analyzing the resonant switched-capacitor circuit, we would like to emphasize that it is not difficult to transfer charge among capacitors with efficiencies over 95% in pure switched-capacitor circuits.

4.3. Energy Analysis in the Resonant Charge Interchange

Recently, many SC topologies have been studied with a resonant charge interchange, with a relatively large efficiency at a relatively large power [40–45,102–116], some of them for a large power [44], which seems unexpected considering SC circuits have these "discharging losses". This is because when the resonant charge interchange is introduced,

the difference in the stored energy that we have called the discharging losses seems to disappear. This has been studied and proven, e.g., in [43]. Here, we present different proof based on the volts-second balance and charge conservation principles, which may be simpler to understand by readers involved in the power electronics field.

Figure 22 shows a resonant switched-capacitor cell. It has a switch that connects the capacitors through the resonant inductor "L_{res}" (small size).
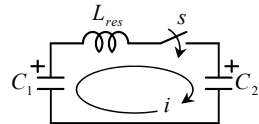
Figure 22. A basic resonant switched-capacitor circuit.

The charge interchange is different than the pure SC case. The main differences are that *(i)* the current tends to be sinusoidal, and *(ii)* we can stop the current before it finds an equilibrium (preferably during a zero crossing), meaning the final voltage of capacitors would be different $v_{1f} \neq v_{2f}$. In other words, the inductor is chosen in a way that the current has a resonant behavior. This requires a very small inductor, much smaller than the energy storage inductors. If we let the circuit reach the equilibrium, parasitic resistances would damp the current, and it will become zero when capacitors are charged to the same voltage, which would lead to the same result of pure switched-capacitor circuits. However, we can also open the switch before that happens. When capacitors have different voltages, the most common choice is to allow only a half-sine wave in the current, which leads to a current as shown in Figure 19, which is more detailed in Figure 23.

Figure 23. Voltage and current signals during the resonant charge interchange.

The current through the inductor starts rising when the switch closes, at an instantaneous rate of $(v_{1i} - v_{2i})/L$; the current of the inductor stops rising when both capacitors have the same voltage, that is, the moment in which the inductor has its maximum current I_{max}, see Figure 23.

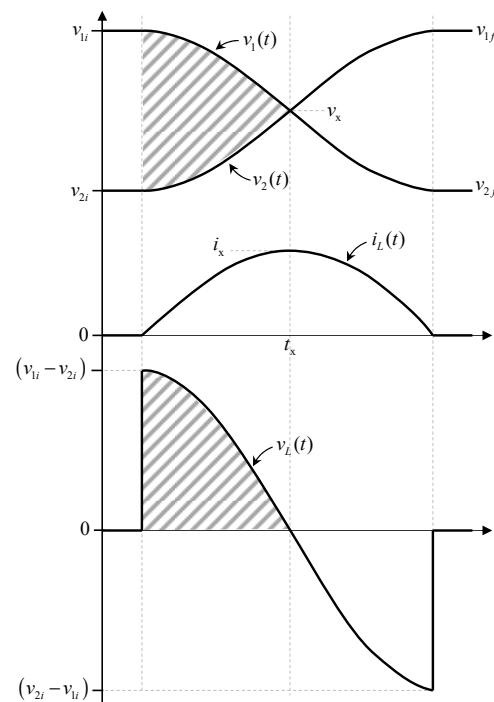During the x-point or maximum current point, the voltage in both capacitors is the same, and it can be called v_x. The voltage v_x can be calculated by using the principle of charge conservation, with the same procedure as in (2), in other words:

$$v_x = \frac{C_1 v_{1i} + C_2 v_{2i}}{C_1 + C_2} \tag{8}$$

We can also calculate the amount of charge that capacitors have interchanged from the beginning of the transient to the x-point. The amount of charge C_1 has transferred to C_2 can be expressed as (9).

$$\Delta_q = C_1 v_{1i} - C_1 v_x = C_1(v_{1i} - v_x) \tag{9}$$

In other words, from the beginning of the transient to the x-point, C_1 has provided charge (it has lost charge), and the amount of lost charge reduces their voltage from v_{1i} to v_x. Again, we are considering that C_1, initially, has a larger voltage; on the other hand, C_2 has gained some charge, the same amount of charge, which can be expressed as (10).

$$\Delta_q = C_2 v_x - C_2 v_{2i} = C_2(v_x - v_{2i}) \tag{10}$$

Note that we consider that C_2 has gained some charge, and its voltage has increased, meaning that v_x is larger than v_{2i}.

In Figure 23, we assumed that both capacitors have the same capacitance, which makes the figure symmetrical, but the equations can be applied to different capacitances.

The inductor was initially discharged. It had zero current at the beginning of the transient, and now, at the x-point, it has its maximum current $I_{max} = I_x$. From the principle of volts per second balance, to discharge the capacitor back to zero current, the same number of volts per second must be applied with inverse polarity, and it will drain the same amount of current in the discharge process (the end of the first half cycle of the shape of the current) compared to the current drained during the charging process.

This means that at the end of the resonant charge interchange (at the end of the semi-sine), capacitor C_1 would lose twice the charge expressed in (9) and (10), and their final charge can be expressed as (11)

$$C_1 v_{1f} = C_1 v_{1i} - 2(C_1 v_{1i} - C_1 v_x) = 2C_1 v_x - C_1 v_{1i} \tag{11}$$

where $C_1 v_{1f}$ is the final charge in C_1, expressed as the initial charge minus the charge lost during the transient (twice the charge expressed in (9)). An analog procedure can be used to calculate the final charge in C_2, their initial charge plus twice the charge it wined (expressed in (10) and (12)).

$$C_2 v_{2f} = C_2 v_{2i} + 2(C_2 v_x - C_2 v_{2i}) = 2C_2 v_x - C_2 v_{2i} \tag{12}$$

By substituting (8) into (11) and (12), the final charge in C_1 and C_2 can be expressed as (13) and (14), respectively.

$$C_1 v_{1f} = 2C_1 \left(\frac{C_1 v_{1i} + C_2 v_{2i}}{C_1 + C_2} \right) - C_1 v_{1i} \tag{13}$$

$$C_2 v_{2f} = 2C_2 \left(\frac{C_1 v_{1i} + C_2 v_{2i}}{C_1 + C_2} \right) - C_2 v_{2i} \tag{14}$$

Let us consider for a moment that both capacitors have the same capacitance ($C_1 = C_2 = C$), then (13) and (14) would lead, respectively, to (15) and (16).

$$C v_{1f} = 2C \left(\frac{C v_{1i} + C v_{2i}}{C + C} \right) - C v_{1i} \Rightarrow v_{1f} = 2 \left(\frac{v_{1i} + v_{2i}}{2} \right) - v_{1i} = v_{2i} \tag{15}$$

$$Cv_{2f} = 2C \left(\frac{Cv_{1i} + Cv_{2i}}{C + C} \right) - Cv_{2i} \Rightarrow v_{2f} = 2 \left(\frac{v_{1i} + v_{2i}}{2} \right) - v_{2i} = v_{1i} \tag{16}$$

Equations (15) and (16) bring an interesting fact. If the capacitors have the same capacitance, the capacitors swap their voltage, and the final voltage in C_1 is equal to the initial voltage in C_2, and vice-versa.

Equations (15) and (16) can be used to demonstrate that there is no difference from the initial stored energy to the final stored energy (there are no discharging losses as in the pure SC circuits); both the initial and final stored energy can be expressed as (17).

$$\varepsilon_i = \frac{Cv_{1i}^2}{2} + \frac{Cv_{2i}^2}{2} = \varepsilon_f = \frac{Cv_{1f}^2}{2} + \frac{Cv_{2f}^2}{2} \tag{17}$$

The conclusion is interesting, but this applies only to the case when capacitors have the same capacitance. The case when capacitors are different leads to the same result (as will be shown). There is no difference between the initial and final stored energy; to demonstrate that, let us consider that the capacitance C_1 is different from C_2, and let us define a ratio among the capacitances (18).

$$k = \frac{C_2}{C_1} \tag{18}$$

By considering (18), Equations (13) and (14) can be rewritten as (19) and (20).

$$C_1 v_{1f} = 2C_1 \left(\frac{C_1 v_{1i} + kC_1 v_{2i}}{C_1 + kC_1} \right) - C_1 v_{1i} \tag{19}$$

$$kC_1 v_{2f} = 2kC_1 \left(\frac{C_1 v_{1i} + kC_1 v_{2i}}{C_1 + kC_1} \right) - kC_1 v_{2i} \tag{20}$$

The definition of k in (18) allows for simplifying the mathematical procedure. Only one capacitance, C_1, is present in equations, which allows simplifying (19) and (20) as (21) and (22), respectively.

$$v_{1f} = 2 \left(\frac{v_{1i} + kv_{2i}}{1 + k} \right) - v_{1i} = \frac{1 - k}{1 + k} v_{1i} + \frac{2k}{1 + k} v_{2i} \tag{21}$$

$$v_{2f} = 2 \left(\frac{v_{1i} + kv_{2i}}{1 + k} \right) - v_{2i} = \frac{2}{1 + k} v_{1i} - \frac{1 - k}{1 + k} v_{2i} \tag{22}$$

Let us consider the following definitions for the sake of simplicity:

$$\alpha = \frac{1 - k}{1 + k} \tag{23}$$

$$\beta = \frac{2}{1 + k} \tag{24}$$

Equations (21) and (22) can be re-written, considering (23) and (24), as (25) and (26).

$$v_{1f} = \alpha v_{1i} + k\beta v_{2i} \tag{25}$$

$$v_{2f} = \beta v_{1i} - \alpha v_{2i} \tag{26}$$

The initial stored energy in the capacitors can be expressed as (27).

$$\varepsilon_i = \frac{C_1 v_{1i}^2}{2} + \frac{C_2 v_{2i}^2}{2} = \frac{C_1}{2} \left(v_{1i}^2 + kv_{2i}^2 \right) \tag{27}$$

while the final energy can be expressed as (28).

$$\varepsilon_f = \frac{C_1 v_{1f}{}^2}{2} + \frac{C_2 v_{2f}{}^2}{2} \tag{28}$$

Now we can substitute (25) and (26) into (28) to investigate if the result is equal to (27).

$$\varepsilon_f = \frac{C_1}{2}(\alpha v_{1i} + k\beta v_{2i})^2 + \frac{C_2}{2}(\beta v_{1i} - \alpha v_{2i})^2 \tag{29}$$

Expanding the quadratic terms in (29) and considering $C_2 = kC_1$ leads to (30).

$$\varepsilon_f = \frac{C_1}{2}\left(\alpha^2 v_{1i}{}^2 + 2k\alpha\beta v_{1i}v_{2i} + k^2\beta^2 v_{2i}{}^2\right) + \frac{kC_1}{2}\left(\beta^2 v_{1i}{}^2 - 2\beta\alpha v_{1i}v_{2i} + \alpha^2 v_{2i}{}^2\right) \tag{30}$$

Multiplying by $2/C_1$ on both sides of (30) leads to (31)

$$\frac{2\varepsilon_f}{C_1} = \left(\alpha^2 v_{1i}{}^2 + 2k\alpha\beta v_{1i}v_{2i} + k^2\beta^2 v_{2i}{}^2\right) + k\left(\beta^2 v_{1i}{}^2 - 2\alpha\beta v_{1i}v_{2i} + \alpha^2 v_{2i}{}^2\right) \tag{31}$$

Now we can group similar terms as in (32).

$$2\frac{\varepsilon_f}{C_1} = v_{1i}{}^2\left[\alpha^2 + k\beta^2\right] + v_{1i}v_{2i}[2k\alpha\beta - 2k\alpha\beta] + v_{2i}{}^2\left[k^2\beta^2 + k\alpha^2\right] \tag{32}$$

The factor that multiplies $v_{1i}{}^2$ can be simplified as (33).

$$\alpha^2 + k\beta^2 = \left(\frac{1-k}{1+k}\right)^2 + k\left(\frac{2}{1+k}\right)^2 = 1 \tag{33}$$

The factor that multiplies $v_{2i}{}^2$ can be simplified as (34):

$$k^2\beta^2 + k\alpha^2 = k^2\left(\frac{2}{1+k}\right)^2 + k\left(\frac{1-k}{1+k}\right)^2 = k \tag{34}$$

The factor that multiplies $v_{1i}v_{2i}$ is:

$$2k\alpha\beta - 2k\alpha\beta = 0 \tag{35}$$

By substituting (33), (34), and (35) into (32), the stored energy in the capacitors after the charge interchange transient can be expressed as (36).

$$2\frac{\varepsilon_f}{C_1} = v_{1i}{}^2 + kv_{2i}{}^2 \quad \Rightarrow \quad \varepsilon_f = C_1\frac{v_{1i}{}^2}{2} + kC_1\frac{v_{2i}{}^2}{2} \tag{36}$$

The stored energy at the end of the charge interchange transient equals the initial stored energy calculated in (27). The conclusion of this exercise is also interesting, and there are no discharge losses. The initial energy is equal to the final energy in a resonant switched-capacitor circuit. That does not mean the energy conversion can be made with 100% of the efficiency as there are still losses in the transistors, switching and conduction losses, as well as in all components of the converter, but the discharging losses that we analyzed for the pure switched capacitors in the former section are not present in resonant switched capacitors.

This result is also because we opened the switch (see Figure 19 or Figure 22) when the current has a zero crossing after the first half sine cycle. This may be challenging since the tolerance of the components may produce small changes in the resonant frequency from one converter to another one. Some solutions have been proposed to overcome this challenge, such as the use of diodes or thyristors to ensure the current will stop at the zero crossing [40,44,45].

4.4. Simulation of the Energy Recovery Phenomena

Computer simulations help us to perform fast analysis of physical systems, and they are widely used in the field of power converters. This section presents a brief simulation of a resonant SC circuit. The intention is to have a quick idea about the stored energy behavior and to have some parameters which can be quickly replied in commercial software. The computer simulations applied to the dc–dc converters are a research field by itself; different approaches and commercial software may bring slightly different results and simulation times due to their convergence [118]. The simulation results discussed in this section were performed using the *Synopsys Saber* software (Version 4.0, Synopsys Inc., Mountain View, CA, USA).

The schematic is shown in Figure 24a, along with the main parameters. Two capacitors of 0.2 F are connected in parallel with different initial voltages. An ideal diode (no voltage drop) was inserted to prevent the current from becoming negative. The diode is ideal, but the inductor has a small equivalent series resistance (*ESR* = 0.001) not shown in the schematic, only to prevent errors in the numerical simulation.
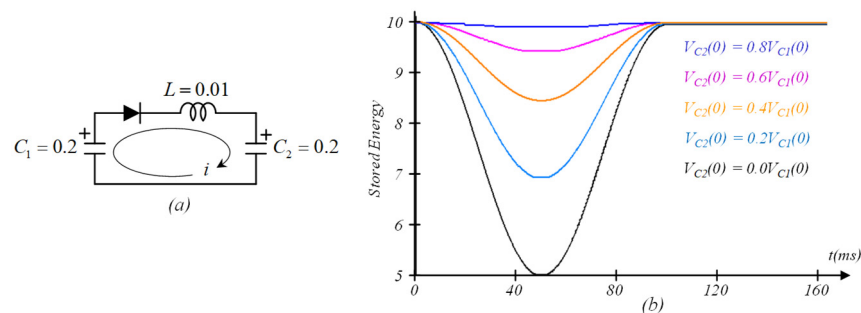
Figure 24. Basic resonant SC circuit simulated, (**a**) schematic with parameters in the simulation, (**b**) evolution of store energy during charge interchange for different values of initial voltage.

Five simulations were performed with an end time of 0.2 s, and a time step of 1 μs. The initial condition or initial voltages in the capacitors are calculated to have 10 Joules (initially). The ratio between the initial voltage in C_2 over the initial voltage in C_1 are: 0, 0.2, 0.4, 0.6, and 0.8. The specific voltages are listed in Table 3.

Table 3. Parameters of simulation in Figure 24b.

$v_{C1}(0)$	$v_{C2}(0)$	$i_L(0)$	Initial Stored Energy
10	0	0	10
9.80581	1.96116	0	10
9.28477	3.71391	0	10
8.57493	5.14496	0	10
7.80869	6.24695	0	10

The results graphics are shown in Figure 24b. The stored energy in the capacitors decreases until it reaches the value predicted by (5). That would be the final stored energy in a pure switched-capacitor circuit. It can be compared to Figure 21. However, after a time, the energy (stored in the inductor) is returned to the capacitors.

5. Hybrid SC Converters

5.1. The Traditional Boost Converters with an Input SC Multiplier

For achieving a large voltage-gain conversion, a traditional boost converter may work at a relatively high duty cycle, but the efficiency of a traditional boost converter (in their simple topology or interleaving) decreases when their duty cycle approaches one.

This constrains the voltage gain achievable with a boost converter [46]. Most switched-capacitor converters are mostly voltage multipliers without output voltage regulation, despite regulations that can be achieved with pure SC converters. Combining SC converters with traditional converters results in a good solution to achieve a high voltage gain and regulation. One approach may be connecting an SC converter in a cascaded connection with a boost converter, which means the output of the SC converter is the input of the boost converter. The topology of the *Series-Parallel Converter* followed by the *Boost Converter* has been investigated in several configurations [51–101], see Figure 25.
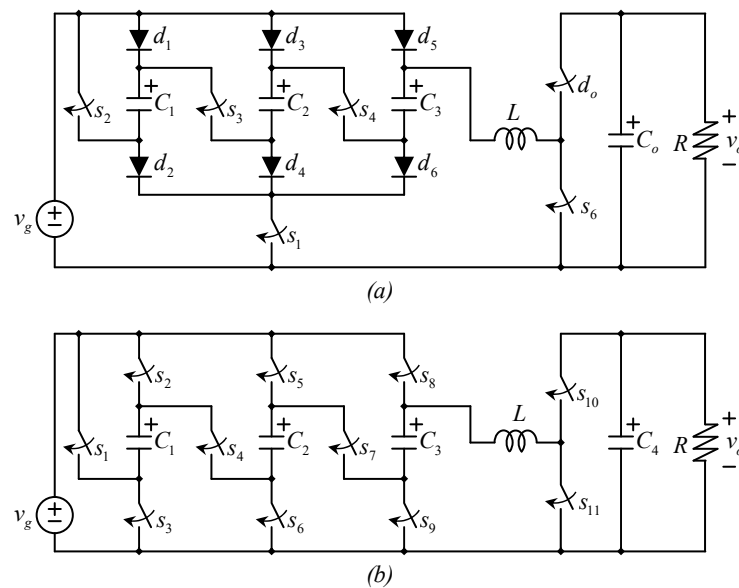
Figure 25. Transistors-based series parallel SC converters in the literature, (**a**) circuit studied in [47,48], (**b**) circuit studied in [49].

The switch realization can be done in different options [9]. This helps to synthesize the converter with different configurations. Figure 25a,b have the same equivalent circuits. Those circuits correspond to references [47–49]; other two similar converters were presented at [50].
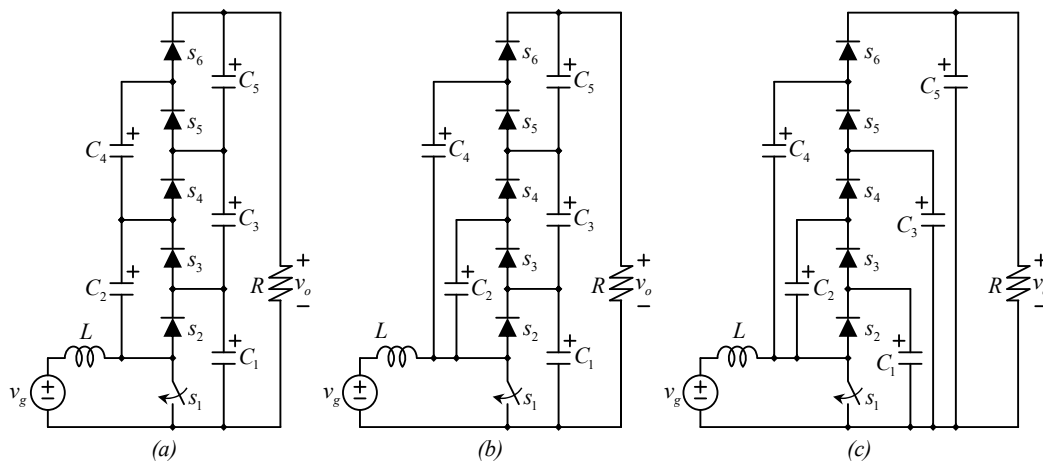
5.2. The Traditional Boost Converters with an Output SC Multiplier

Instead of connecting an SC circuit as the input of a boost converter, an SC circuit can be connected as the output of a boost converter. This brings the topology of the multilevel boost converter [51], a converter that drives a voltage multiplier such as the ones in Figure 3 with a boost converter. Any of the voltage multipliers in Figure 3 can be used for this purpose. Figure 26 shows three possible options.

The multilevel boost converter has been studied in several articles [51–59], with contributions that include their modeling and control [56–59]. Some works include the negative extension (instead of the positive) or both [51,55,57].

The multilevel boost converter has several advantages which make it very attractive. It requires only one transistor rated to a relatively low voltage, all the diodes and the transistors are rated to the same voltage, depending on the voltage multiplier, i.e., in Figure 26a, and all capacitors are rated to the same voltage, which is relatively low compared to the output voltage. The input current is continuous, and the transistor is grounded, simplifying the gate drive design. As shown in [41], only one tiny capacitor is required to achieve the resonant charge interchange in all capacitors.

Figure 26. The Multilevel boost converter: (**a**) topology studied in [51], (**b**) topology studied in [52], (**c**) topology studied in [41].

5.3. Other Traditional Converters with SC Voltage Multipliers

As well as to the boost converter, other traditional topologies can be used to drive a diode-capacitor voltage multiplier. Figure 27a shows the traditional Cuk converter. Figure 27b shows the multiplier Cuk Converter. Figure 27c shows the traditional Single-Ended Primary-Inductor Converter or SEPIC, while Figure 27d illustrates their multiplier version. Those converters have been studied in [60,61].
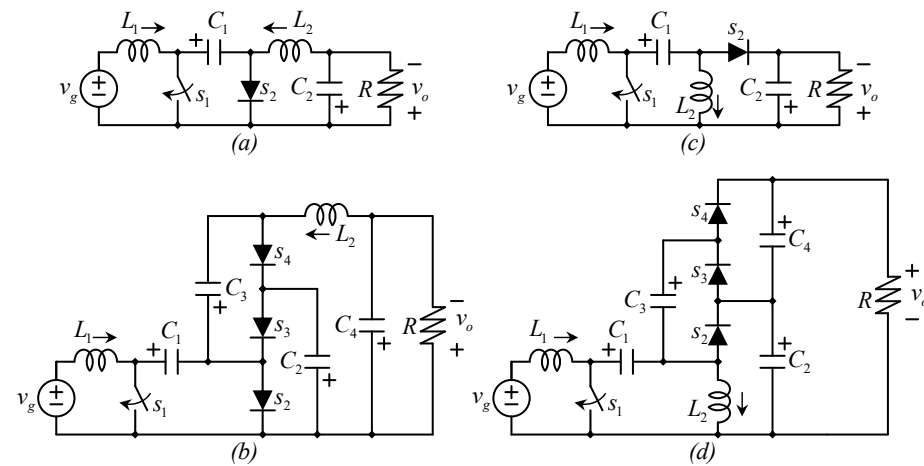
Figure 27. Other traditional converters and their multiplier version: (**a**) the Cuk converter, (**b**) multiplier Cuk converter [60], (**c**) the SEPIC converter, and (**d**) multiplier SEPIC converter [61].

Other configurations have been investigated based on the same principle for either a dc input [62–66] or an ac input [67–69].

Other configurations have been tried with more than one input switching state, for example, with two interleaved switching stages to drive a ladder voltage multiplier [70–85]; some of those topologies resemble the series capacitor boost converter.

Another possibility is using the quadratic boost converter to drive the voltage multiplier, as explored in [90,91], or topologies with multiple inductors [92–95], Z-source networks [96,97], and the cascaded connection or the interconnection with sets of multipliers in different manners [98–101].

5.4. Traditional SC Converters Modified to Have Resonant Charge Interchange

Several studies have been dedicated to the use of traditional SC topologies for power conversion with a resonant charge interchange. One example is the ladder converter with

the resonant charge interchange shown in Figure 28. Figure 28a shows the 2× multiplier (the output voltage is twice the input), while Figure 28b shows the 4× converter.
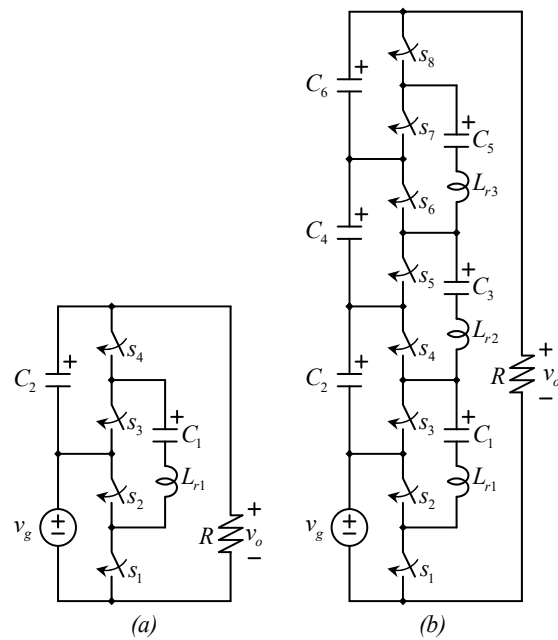
Figure 28. The resonant ladder SC converter, (**a**) 2× version, (**b**) 4× version.

This converter has been used in several applications, mainly for voltage equalization in a series of capacitors or batteries [102–106]. The resonant charge interchange can be produced in a traditional SC converter by introducing small inductors in some parts of the circuit.

The multilevel boost converter, see Figure 26, or multiplier boost converter has also been studied in their resonant charge interchange version [41], see Figure 29.

Figure 29. The Multilevel boost converter with resonant charge interchange [41].

A modified version of the converter in Figure 9 has been investigated in [107] (see Figure 30). It consists of a cascaded connection of two converters with convenient modifications to produce a resonant charge interchange.

Figure 30. A resonant version of the converter in Figure 9.
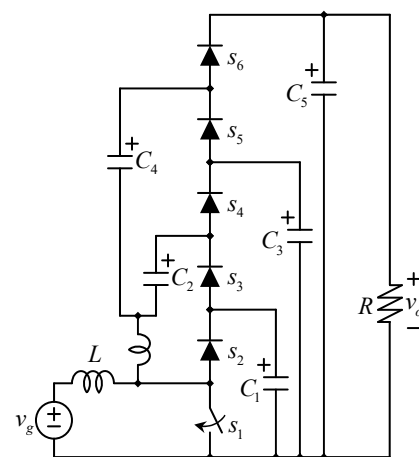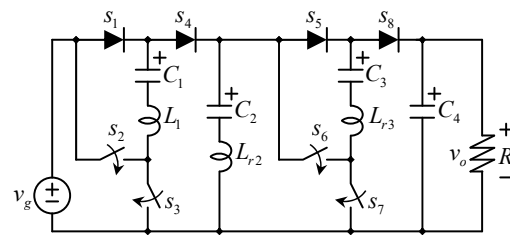
A modified version of the Series-Parallel converter, see Figure 10, was studied in [44], with a resonant charge interchange, as shown in Figure 31. Figure 31a shows the straight-forward converter with thyristors and diodes, while Figure 31b shows a simplified version proposed in [44] with fewer switches but the same operation.

(a)

(b)
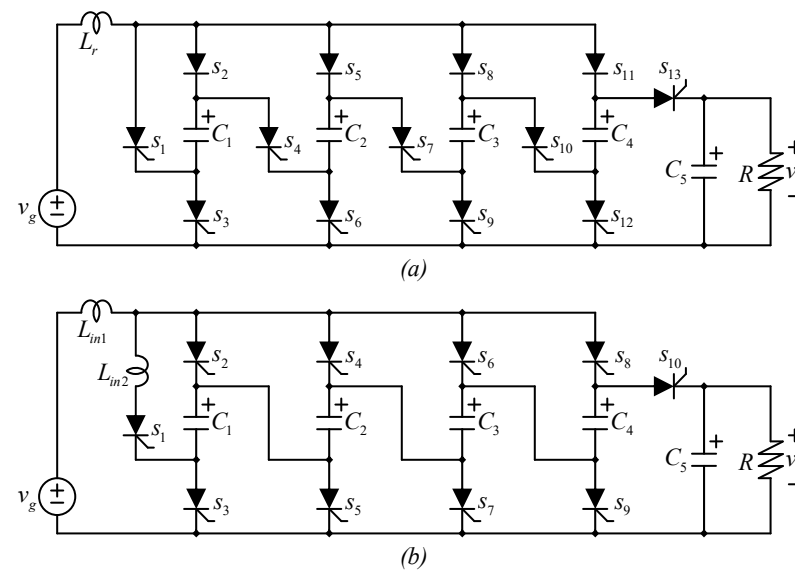
Figure 31. Thyristors-based implementations of the series-capacitor SC converter with resonant charge interchange, (**a**) straight forward realization, (**b**) a simplified version proposed in [44].

Thyristors can be used to produce the resonant charge interchange and stop the current automatically when it tries to become negative, particularly useful in very large power applications, such as the one presented in [44] (see Figure 31).

The Fibonacci SC topology, see Figure 11, was used in [40] with the resonant charge interchange. The contribution included a modified switching sequence that allows performing the resonant charge interchange with a single inductor.

The Flying Capacitor topology, see Figure 13, has been used as a traditional dc–dc converter, with a stored energy inductor and PWM voltage regulation, and also a SC converter with a resonant charge interchange [30]. Another resonant charge interchange SC converter was recently studied in [108].

The SC converter shown in Figure 6 was studied with a resonant charge interchange (with a single inductor) in [109], and the topology is shown in Figure 32.

Figure 32. Topology studied in [109].

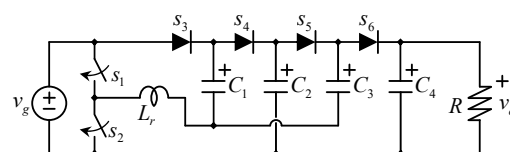The MMCC converter, see Figure 15, has been studied in their resonant charge interchange version [110,111]. In this case, the authors proposed not to use physical inductors, but to use the distributed inductance on the circuit to produce the resonant operation. Other topologies which are different from the traditional have been studied to achieve SC power conversion with a resonant charge interchange [112–116].

5.5. Demonstrative Experimental Results

As a demonstrative example, a traditional multilevel boost converter was built. The experimental results are provided in this section. Figure 33 shows the 2× multilevel (or multiplier) boost converter, Figure 33a shows the circuit schematic, while Figure 33b,c show the equivalent circuits of the converter when the switch is closed and open, respectively.
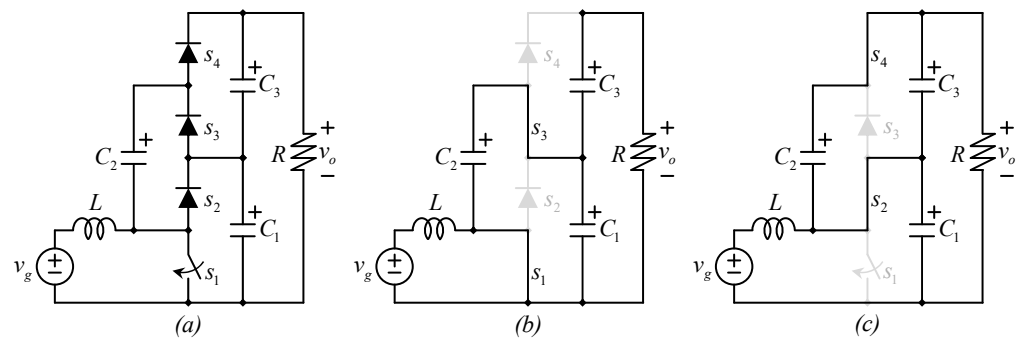

Figure 33. A 2× multilevel boost converter, (**a**) schematic, (**b**) equivalent circuit when the transistor is closed, and (**c**) equivalent circuit when the transistor is open.

When the transistor is closed, the inductor is connected to the input voltage v_g, when the switch opens, the voltage across the inductor is $v_g - v_{C1}$. From the circuits shown in Figure 33, and by applying the averaging theory [9], it is possible to write the inductor voltage along the entire switching period, as in (37).

$$\frac{d}{dt} i_L = d \frac{v_g}{L} + (1-d) \frac{v_g - v_{C1}}{L} \tag{37}$$

where d is the duty cycle of the converter, i.e., the time in which the converter is closed divided by the total switching period. By considering the small ripple approximation and the steady state condition [9], it is possible to obtain the voltage across the capacitor and express it in terms of the duty cycle and the input voltage. The steady state or equilibrium voltage across C_1 can be expressed as (38).

$$V_{C1} = \frac{V_g}{1-D} \tag{38}$$

The use of upper-case letters indicates steady state (or equilibrium) values. From Equation (38), we can see that capacitor C_1 has the same voltage of a traditional boost converter. Then, we can see from Figure 33b, that there is a switched-capacitor action in which capacitor C_1 transfers charge to capacitor C_2. This is a non-resonant charge interchange. Despite this, the charge interchange may lead to discharging losses. If the voltage in C_2 is 65% of the voltage in C_1 before it is in parallel, the efficiency of the charge interchange would be around 95% (see Figure 21). At the next switching action, C_2 transfers charge to C_3, in a similar action. The amount of charge transferred from C_2 to C_3 can be calculated as (39).

$$\Delta q_{C2 \text{ to } C3} = I_{out} D \frac{1}{f_S} \tag{39}$$

where f_S represents the switching frequency. Equation (39) calculates the amount of charge lost by C_3 when the switch is off, and this charge must be recovered from C_2 in a steady

state. The voltage drop in C_3 can be calculated by dividing the charge in (39) over the capacitance C_3. This amount of charge transferred from C_2 to C_3 comes from C_1 when the switch is closed, and then the same calculation can be performed to calculate the voltage drop in the capacitor C_2. Table 4 contains the experiment parameters.

Table 4. Parameters of simulation in Figure 24a.

Capacitance of Capacitors $C_1 = C_2 = C_3$	10 μF
Inductance L	1 mH
MOSFET	*IRFP4127PbF*
Diodes (all 3)	*APT60S20BG*
Switching frequency	50 kHz
Output load resistor R	100 Ω

Figure 34 shows important waveforms, the current through the inductor, the output voltage (voltage across the resistor), the voltage across C_1, and the switch voltage; the voltages are displayed at 50 V/div and the current at 1 A/div. Figure 34a corresponds to an input voltage of $v_g = 50$ V and a duty cycle of $D = 0.5$, the output voltage was measured as 189 V, the output power measured as 357 W, and the efficiency as 93%. Figure 34b corresponds to the operating point in which the input voltage $v_g = 50$ V, the duty cycle was $D = 0.6$, the output voltage was measured as 238 V, the output power measured as 362 W, and the efficiency was 93%.

(**a**)

(**b**)
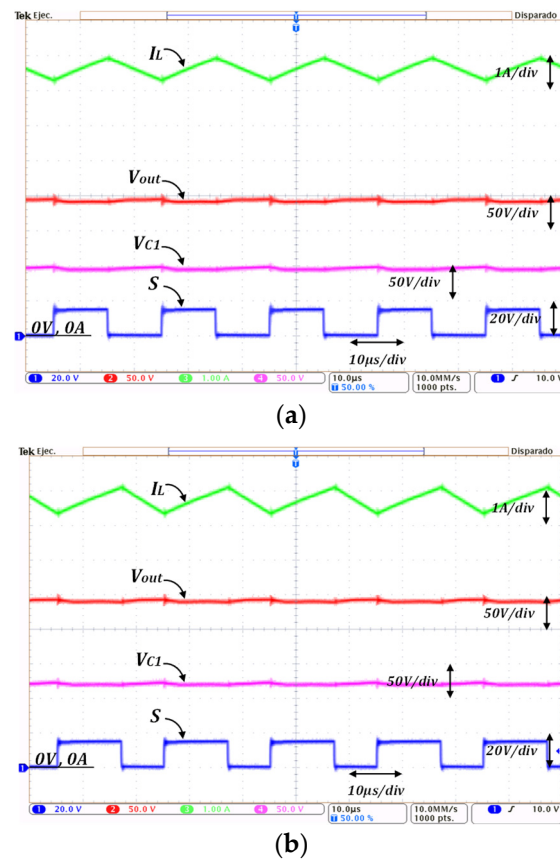
Figure 34. Important waveforms of the converter operation, from top to bottom: the current through the inductor, the output voltage, the voltage across capacitor C_1 and switch voltage. (**a**) For $D = 0.5$, and (**b**) for $D = 0.6$.

Figure 35 corresponds to the operating point in which the input voltage v_g = 50 V, the duty cycle was D = 0.7, the output voltage was measured as 321 V, the output power was measured as 371 W, and the efficiency as 94%.
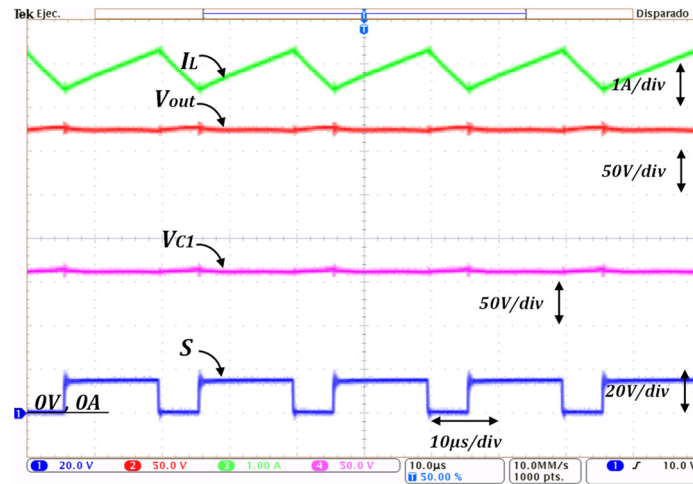
Figure 35. Important waveforms of the converter operation, from top to bottom: the current through the inductor, the output voltage, the voltage across capacitor C_1, and switch voltage for D = 0.7.

6. Conclusions

This article presents an overview of hybrid SC converters. It starts with a short review of pure SC circuits, but then it focuses on modifications of those circuits, mainly with the use of small resonant inductors, which leads to resonant SC circuits, and their combination of traditional converters such as the boost converter.

The resonant charge interchange is a relatively new tendency among designers of SC circuits. It is relevant since several converters have been investigated with a relatively large efficiency. The overview includes topologies recently introduced to the state-of-the-art. Particularly, converters under study are non-isolated and unidirectional in terms of power flow; most of them can be adapted to provide bidirectional power flow, with the cost of increasing the number of transistors.

In addition to the overview, which is the article's main contribution, an analysis is presented to explain the discharging losses, a difference between the initial and final amount of stored energy in capacitors when connected in parallel. The analysis presented in this article explains this phenomenon and how to ensure discharging losses are less than a particular percentage. Furthermore, one element of proof is provided to demonstrate that no losses are present due to the discharging phenomenon when the transferred energy is resonant. The provided proof is different from other proofs presented in the literature, and it is based on the amperes per second and charge conservation principles. Those bases are very well understood by power electronics engineers, which improves the knowledge of this phenomenon.

Author Contributions: Authors J.C.R.-C. and J.C.M.-M. contributed with the conceptualization of the article; J.E.V.-R. and A.A.-R. contributed with the methodology; F.B.-C. contributed with the software, validation, and formal analysis; O.L.-S. and J.C.R.-C. wrote the draft and manuscript preparation. All authors have read and agreed to the published version of the manuscript.

Institutional Review Board Statement: Not applicable.

Informed Consent Statement: Not applicable.

References

1.   Lew, D.; Bakke, J.; Bloom, A.; Brown, P.; Caspary, J.; Clack, C.; Miller, N.; Orths, A.; Silverstein, A.; Simonelli, J.; et al. Transmission Planning for 100% Clean Electricity: Enabling Clean, Affordable, and Reliable Electricity. *IEEE Power Energy Mag.* **2021**, *19*, 56–66. [CrossRef]

2.   Holttinen, H.; Groom, A.; Kennedy, E.; Woodfin, D.; Barroso, L.; Orths, A.; Ogimoto, K.; Wang, C.; Moreno, R.; Parks, K.; et al. Variable Renewable Energy Integration: Status Around the World. *IEEE Power Energy Mag.* **2021**, *19*, 86–96. [CrossRef]

3.   O'Malley, M.; Bowen, T.; Bialek, J.; Braun, M.; Cutululis, N.; Green, T.; Hansen, A.; Kennedy, E.; Kiviluoma, J.; Leslie, J.; et al. Enabling Power System Transformation Globally: A System Operator Research Agenda for Bulk Power System Issues. *IEEE Power Energy Mag.* **2021**, *19*, 45–55. [CrossRef]

4.   O'Connell, R.; Phadke, A.; O'Boyle, M.; Clack, C.T.; Denholm, P.; Ernst, B. Carbon-Free Energy: How Much, How Soon? *IEEE Power Energy Mag.* **2021**, *19*, 67–76.

5.   Jana, A.S.; Lin, C.-H.; Kao, T.-H.; Chang, C.-H. A High Gain Modified Quadratic Boost DC–DC Converter with Voltage Stress Half of Output Voltage. *Appl. Sci.* **2022**, *12*, 4914. [CrossRef]

6.   Pesce, C.; Riedemann, J.; Peña, R.; Degano, M.; Pereda, J.; Villalobos, R.; Maury, C.; Young, H.; Andrade, I. A Modified Multi-Winding DC–DC Flyback Converter for Photovoltaic Applications. *Appl. Sci.* **2021**, *11*, 11999. [CrossRef]

7.   Alavi, O.; Rajabloo, T.; De Ceuninck, W.; Daenen, M. Non-Isolated DC–DC Converters in Fuel Cell Applications: Thermal Analysis and Reliability Comparison. *Appl. Sci.* **2022**, *12*, 5026. [CrossRef]

8.   Lopez-Caiza, D.; Renaudineau, H.; Muller, N.; Flores-Bahamonde, F.; Kouro, S.; Rodriguez, J. Dual-Boost Inverter for PV Microinverter Application—An Assessment of Control Strategies. *Appl. Sci.* **2022**, *12*, 5952. [CrossRef]

9.   Erickson, R.W.; Maksimovic, D. *Fundamentals of Power Electronics*, 2nd ed.; Kluwer: Boston, MA, USA, 2004.

10. Rashid, M. *Power Electronics: Circuits, Devices and Applications*, 3rd ed.; Prentice Hall: London, UK, 2004.

11. Undeland, M.N.; Robbins, W.P.; Mohan, N. Power Electronics. In *Converters, Applications, and Design*, 3rd ed.; John Whiley & Sons: Hoboken, NJ, USA, 1995.

12. Kazmierkowski, M.P.; Krishnan, R.; Blaabjerg, F. *Control in Power Electronics Selected Problems*; Academic Press: Cambridge, MA, USA, 2002.

13. de Souza, A.; Tofoli, F.; Ribeiro, E. Switched Capacitor DC–DC Converters: A Survey on the Main Topologies, Design Characteristics, and Applications. *Energies* **2021**, *14*, 2231. [CrossRef]

14. Tanzawa, T. Innovation of Switched-Capacitor Voltage Multiplier: Part 1: A Brief History. *IEEE Solid State Circuits Mag.* **2016**, *8*, 51–59. [CrossRef]

15. Tanzawa, T. Innovation of Switched-Capacitor Voltage Multiplier: Part 2: Fundamentals of the Charge Pump. *IEEE Solid State Circuits Mag.* **2016**, *8*, 83–92. [CrossRef]

16. Tanzawa, T. Innovation of Switched-Capacitor Voltage Multiplier: Part 3: State of the Art of Switching Circuits and Applications of Charge Pumps. *IEEE Solid State Circuits Mag.* **2016**, *8*, 63–73. [CrossRef]

17. Falkner, A. Generalised Cockcroft-Walton voltage multipliers. *Electron. Lett.* **1973**, *9*, 585–586. [CrossRef]

18. Dickson, J. On-chip high-voltage generation in MNOS integrated circuits using an improved voltage multiplier technique. *IEEE J. Solid State Circuits* **1976**, *11*, 374–378. [CrossRef]

19. Brugler, J. Theoretical performance of voltage multiplier circuits. *IEEE J. Solid State Circuits* **1971**, *6*, 132–135. [CrossRef]

20. Makowski, M.S.; Maksimovic, D. Performance limits of switched-capacitor DC–DC converters. In Proceedings of the PESC 1995, Power Electronics Specialist Conference, Atlanta, GA, USA, 18–22 June 1995; pp. 1215–1221.

21. Ueno, F.; Inoue, T.; Oota, I.; Harada, I. Emergency power supply for small computer systems. In Proceedings of the IEEE In-ternational Sympoisum on Circuits and Systems, Singapore, 11–14 June 1991; pp. 1065–1068.

22. Rosas-Caro, J.C.; Ramirez, J.M.; Vite, P.M.G. A novel two switches based DC–DC multilevel voltage multiplier. In Proceedings of the 2008 International Symposium on Power Electronics, Electrical Drives, Automation and Motion, Ischia, Italy, 11–13 June 2008; pp. 930–934. [CrossRef]

23. Lopez, A.; Diez, R.; Perilla, G.; Patino, D. Analysis and Comparison of Three Topologies of the Ladder Multilevel DC/DC Converter. *IEEE Trans. Power Electron.* **2012**, *27*, 3119–3127. [CrossRef]

24. Daowd, M.; Antoine, M.; Omar, N.; Van den Bossche, P.; Van Mierlo, J. Single Switched Capacitor Battery Balancing System Enhancements. *Energies* **2013**, *6*, 2149–2174. [CrossRef]

25. Li, S.; Zheng, Y.; Wu, B.; Smedley, K.M. A Family of Resonant Two-Switch Boosting Switched-Capacitor Converter with ZVS Operation and a Wide Line Regulation Range. *IEEE Trans. Power Electron.* **2017**, *33*, 448–459. [CrossRef]

26. Bhaskar, M.S.; Padmanaban, S.; Blaabjerg, F. A Multistage DC–DC Step-Up Self-Balanced and Magnetic Component-Free Converter for Photovoltaic Applications: Hardware Implementation. *Energies* **2017**, *10*, 719. [CrossRef]

27. Peng, F.Z.; Zhang, F.; Qian, Z. A novel compact DC–DC converter for 42 V systems. In Proceedings of the IEEE 34th Annual Conference on Power Electronics Specialist, Acapulco, Mexico, 15–19 June 2003; Volume 1, pp. 33–38.

28. Pan, Z.; Zhang, F.; Peng, F.Z. Power losses and efficiency analysis of multilevel dc–dc converters. In Proceedings of the Twentieth Annual IEEE Applied Power Electronics Conference and Exposition, Austin, TX, USA, 06–10 March 2005; Volume 3, pp. 1393–1398.

29. Zhang, F.; Du, L.; Peng, F.Z.; Qian, Z. A New Design Method for High-Power High-Efficiency Switched-Capacitor DC–DC Converters. *IEEE Trans. Power Electron.* **2008**, *23*, 832–840. [CrossRef]

30. Qian, W.; Peng, F.Z.; Shen, M.; Tolbert, L.M. 3X DC–DC Multiplier/Divider for HEV Systems. In Proceedings of the 2009 Twenty-Fourth Annual IEEE Applied Power Electronics Conference and Exposition, Washington, DC, USA, 15–19 February 2009; pp. 1109–1114.

31. Qian, W.; Cha, H.; Peng, F.Z.; Tolbert, L.M. 55-kW Variable 3X DC–DC Converter for Plug-in Hybrid Electric Vehicles. *IEEE Trans. Power Electron.* **2011**, *27*, 1668–1678. [CrossRef]

32. Khan, F.H.; Tolbert, L.M. A Multilevel Modular Capacitor-Clamped DC–DC Converter. *IEEE Trans. Ind. Appl.* **2007**, *43*, 1628–1638. [CrossRef]

33. Qian, W.; Cao, D.; Cintron-Rivera, J.G.; Gebben, M.; Wey, D.; Peng, F.Z. A Switched-Capacitor DC–DC Converter with High Voltage Gain and Reduced Component Rating and Count. *IEEE Trans. Ind. Appl.* **2012**, *48*, 1397–1406. [CrossRef]

34. Ben-Yaakov, S. Behavioral Average Modeling and Equivalent Circuit Simulation of Switched Capacitors Converters. *IEEE Trans. Power Electron.* **2011**, *27*, 632–636. [CrossRef]

35. Cheung, C.-K.; Tan, S.-C.; Tse, C.K.; Ioinovici, A. On Energy Efficiency of Switched-Capacitor Converters. *IEEE Trans. Power Electron.* **2012**, *28*, 862–876. [CrossRef]

36. Jevtic, R.; Le, H.-P.; Blagojevic, M.; Bailey, S.; Asanović, K.; Alon, E.; Nikolic, B. Per-Core DVFS With Switched-Capacitor Converters for Energy Efficiency in Manycore Processors. *IEEE Trans. Very Large Scale Integr. (VLSI) Syst.* **2014**, *23*, 723–730. [CrossRef]

37. Mayo-Maldonado, J.; Rosas Caro, J.C.; Rapsisarada, P. Modeling Approaches for DC–DC Converters with Switched Capaci-tors. *IEEE Trans. Ind. Electron.* **2015**, *62*, 953–959.

38. Ballo, A.; Grasso, A.D.; Palumbo, G. A Review of Charge Pump Topologies for the Power Management of IoT Nodes. *Electronics* **2019**, *8*, 480. [CrossRef]

39. Shin, S.-U.; Hong, S.-W.; Lee, H.-M.; Cho, G.-H. High-Efficiency Hybrid Dual-Path Step-Up DC–DC Converter with Continuous Output-Current Delivery for Low Output Voltage Ripple. *IEEE Trans. Power Electron.* **2020**, *35*, 6025–6038.

40. Rosas-Caro, J.C.; Mayo-Maldonado, J.C.; Mancilla-David, F.; Valderrabano-Gonzalez, A.; Carbajal, F.B. Single-inductor resonant switched capacitor voltage multiplier with safe commutation. *IET Power Electron.* **2015**, *8*, 507–516. [CrossRef]

41. Rosas-Caro, J.C.; Mayo-Maldonado, J.C.; Valderrabano-Gonzalez, A.; Beltran-Carbajal, F.; Ramirez-Arredondo, J.M.; Rodriguez-Rodriguez, J.R. DC–DC multiplier boost converter with resonant switching. *Electr. Power Syst. Res.* **2015**, *119*, 83–90. [CrossRef]

42. Zou, K.; Scott, M.J.; Wang, J. A Switched-Capacitor Voltage Tripler With Automatic Interleaving Capability. *IEEE Trans. Power Electron.* **2011**, *27*, 2857–2868. [CrossRef]

43. Mayo-Maldonado, J.C.; Maupong, T.M.; Valdez-Resendiz, J.E.; Rosas-Caro, J.C. Storage and Dissipation Limits in Resonant Switched-Capacitor Converters. *Math. Probl. Eng.* **2018**, *2018*, 1054179. [CrossRef]

44. Kawa, A.; Stala, R.; Mondzik, A.; Pirog, S.; Penczek, A. High-power thyristor-based dc–dc switched-capacitor voltage multi-pliers: Basic concept and novel derived topology with reduced number of switches. *IEEE Trans. Power Electron.* **2016**, *31*, 6797–6813.

45. Choi, H.; Jang, M. and Pou, J. High-gain soft-switching interleaved switched-capacitor DC–DC converter with phase-shedding technique. *IET Power Electron.* **2017**, *10*, 1013–1022. [CrossRef]

46. Lenk, R. *Practical Design of Power Supplies*; IEEE Press: Piscataway, NJ, USA, 2005. [CrossRef]

47. Abutbul, O.; Gherlitz, A.; Berkovich, Y.; Ioinovici, A. Step-up switching-mode converter with high voltage gain using a switched-capacitor circuit. *IEEE Trans. Circuits Syst. I Regul. Pap.* **2003**, *50*, 1098–1102. [CrossRef]

48. Rodič, M.; Milanovič, M.; Truntič, M.; Ošlaj, B. Switched-Capacitor Boost Converter for Low Power Energy Harvesting Applications. *Energies* **2018**, *11*, 3156. [CrossRef]

49. Ošlaj, B.; Truntič, M. Control of a Modified Switched-Capacitor Boost Converter. *Electronics* **2022**, *11*, 654. [CrossRef]

50. Guo, R.; Liang, Z.; Huang, A.Q. A Family of Multimodes Charge Pump based DC–DC Converter with High Efficiency over Wide Input and Output Range. *IEEE Trans. Power Electron.* **2012**, *27*, 4788–4798. [CrossRef]

51. Rosas-Caro, J.C.; Ramirez, J.M.; Peng, F.Z.; Valderrabano, A. A DC–DC multilevel boost converter. *IET Power Electron.* **2010**, *3*, 129–137. [CrossRef]

52. Uno, M.; Tanaka, K. Single-switch multioutput charger using voltage multiplier for series-connected lithium-ion bat-tery/supercapacitor equalization. *IEEE Trans. Ind. Electron.* **2012**, *60*, 3227–3239. [CrossRef]

53. Park, Y.; Jung, B.; Choi, S. Nonisolated ZVZCS Resonant PWM DC–DC Converter for High Step-Up and High-Power Applications. IEEE Trans. *Power Electron.* **2012**, *27*, 3568–3575. [CrossRef]

54. Iqbal, A.; Sagar Bhaskar, M.; Meraj, M.; Padmanaban, S. DC-Transformer Modelling, Analysis and Comparison of the Experimental Investigation of a Non-Inverting and Non-Isolated Nx Multilevel Boost Converter (Nx MBC) for Low to High DC Voltage Applications. *IEEE Access* **2018**, *6*, 70935–70951. [CrossRef]

55. Rosas-Caro, J.; Garcia-Vite, P.M.; Lozano, J.; Gonzalez-Rodriguez, A.; Castillo-Gutierrez, R.; Castillo-Ibarra, R. Generalized DC–DC multiplier converter topology. *IEICE Electron. Express* **2012**, *9*, 1522–1527. [CrossRef]

56. Mayo-Maldonado, J.; Salas-Cabrera, R.; Rosas-Caro, J.; De Leon-Morales, J.; Salas-Cabrera, E. Modelling and control of a DC–DC multilevel boost converter. *IET Power Electron.* **2011**, *4*, 693–700. [CrossRef]

57. Iqbal, A.; Bhaskar, M.S.; Meraj, M.; Padmanaban, S.; Rahman, S. Closed-Loop Control and Boundary for CCM and DCM of Nonisolated Inverting $N\times$ Multilevel Boost Converter for High-Voltage Step-Up Applications. *IEEE Trans. Ind. Electron.* **2019**, *67*, 2863–2874. [CrossRef]

58. Li, X.; Zhang, X.; Jiang, W.; Wang, J.; Wang, P.; Wu, X. A Novel Assorted Nonlinear Stabilizer for DC–DC Multilevel Boost Converter with Constant Power Load in DC Microgrid. *IEEE Trans. Power Electron.* **2020**, *35*, 11181–11192. [CrossRef]

59. Villarreal-Hernandez, C.A.; Ruiz-Martinez, O.F.; Mayo-Maldonado, J.C.; Escobar, G.; Valdez-Resendiz, J.E.; Rosas-Caro, J.C. Minimum Current Ripple Point Tracking Control for Interleaved Dual Switched-Inductor DC–DC Converters. *IEEE Trans. Ind. Electron.* **2020**, *68*, 175–185. [CrossRef]

60. Rosas-Caro, J.C.; Mayo-Maldonado, J.C.; Salas-Cabrera, R.; Gonzalez-Rodriguez, A.; Salas-Cabrera, E.N.; Castillo-Ibarra, R. A family of DC–DC multiplier converters. *Eng. Lett.* **2011**, *19*, 57–67.

61. Rosas-Caro, J.C.; Sanchez, V.M.; Vazquez-Bautista, R.F.; Morales-Mendoza, L.J.; Mayo-Maldonado, J.C.; Garcia-Vite, P.M.; Barbosa, R. A novel DC–DC multilevel SEPIC converter for PEMFC systems. *Int. J. Hydrog. Energy* **2016**, *41*, 23401–23408. [CrossRef]

62. Prudente, M.; Pfitscher, L.L.; Emmendoerfer, G.; Romaneli, E.F.; Gules, R. Voltage Multiplier Cells Applied to Non-Isolated DC–DC Converters. *IEEE Trans. Power Electron.* **2008**, *23*, 871–887. [CrossRef]

63. Young, C.M.; Chen, M.H.; Chang, T.A.; Ko, C.C.; Jen, K.K. Cascade Cockcroft—Walton Voltage Multiplier Applied to Transformerless High Step-Up DC–DC Converter. *IEEE Trans. Ind. Electron.* **2013**, *60*, 523–537. [CrossRef]

64. Wu, B.; Li, S.; Liu, Y.; Smedley, K.M. A New Hybrid Boosting Converter for Renewable Energy Applications. *IEEE Trans. Power Electron.* **2015**, *31*, 1203–1215. [CrossRef]

65. Tran, V.-T.; Nguyen, M.-K.; Choi, Y.-O.; Cho, G.-B. Switched-Capacitor-Based High Boost DC–DC Converter. *Energies* **2018**, *11*, 987. [CrossRef]

66. Liu, J.; Xu, M.; Zeng, J.; Wu, J.; Eric, C.K.W. Modified voltage equaliser based on Cockcroft–Walton voltage multipliers for series-connected supercapacitors. *IET Electr. Syst. Transp.* **2018**, *8*, 44–51. [CrossRef]

67. Dias, J.C.; Lazzarin, T.B. A Family of Voltage-Multiplier Unidirectional Single-Phase Hybrid Boost PFC Rectifiers. *IEEE Trans. Ind. Electron.* **2017**, *65*, 232–241. [CrossRef]

68. Young, C.-M.; Chen, H.-L.; Chen, M.-H. A Cockcroft–Walton Voltage Multiplier Fed by a Three-Phase-to-Single-Phase Matrix Converter with PFC. *IEEE Trans. Ind. Appl.* **2013**, *50*, 1994–2004. [CrossRef]

69. Guimaraes, J.C.; Cortez, D.F.; Badin, A.A. Single-Phase Hybrid Switched-Capacitor Interleaved AC-DC Boost Converter. *IEEE Access* **2021**, *9*, 140799–140808. [CrossRef]

70. Kim, P.; Lee, S.; Park, J.; Choi, S. High step-up interleaved boost converters using voltage multiplier cells. In Proceedings of the 8th International Conference on Power Electronics-ECCE Asia, Jeju, Korea, 30 May–3 June 2011; pp. 2844–2851. [CrossRef]

71. Tofoli, F.L.; Oliveira, D.D.S.; Torrico-Bascopé, R.P.; Alcazar, Y.J.A. Novel Nonisolated High-Voltage Gain DC–DC Converters Based on 3SSC and VMC. *IEEE Trans. Power Electron.* **2012**, *27*, 3897–3907. [CrossRef]

72. Alcazar, Y.J.A.; Oliveira, D.D.S.; Tofoli, F.L.; Torrico-Bascope, R.P. DC–DC Nonisolated Boost Converter Based on the Three-State Switching Cell and Voltage Multiplier Cells. *IEEE Trans. Ind. Electron.* **2012**, *60*, 4438–4449. [CrossRef]

73. Lee, S.; Kim, P.; Choi, S. High Step-Up Soft-Switched Converters Using Voltage Multiplier Cells. *IEEE Trans. Power Electron.* **2012**, *28*, 3379–3387. [CrossRef]

74. Prabhala, V.A.K.; Fajri, P.; Gouribhatla, V.S.P.; Baddipadiga, B.P.; Ferdowsi, M. A DC–DC Converter with High Voltage Gain and Two Input Boost Stages. *IEEE Trans. Power Electron.* **2015**, *31*, 4206–4215. [CrossRef]

75. Muller, L.; Kimball, J.W. Dual-input high gain DC–DC converter based on the Cockcroft-Walton multiplier. In Proceedings of the 2014 IEEE Energy Conversion Congress and Exposition (ECCE), Pittsburgh, PA, USA, 14–18 September 2014; pp. 5360–5367. [CrossRef]

76. Chen, J.; Wang, C.; Li, J. An Input-Parallel-Output-Series Switched-Capacitor Three-level Boost Converter with a Three-Loop Control Strategy. *Energies* **2018**, *11*, 2631. [CrossRef]

77. Rajaei, A.; Khazan, R.; Mahmoudian, M.; Mardaneh, M.; Gitizadeh, M. A Dual Inductor High Step-Up DC/DC Converter Based on the Cockcroft–Walton Multiplier. *IEEE Trans. Power Electron.* **2018**, *33*, 9699–9709. [CrossRef]

78. Chen, J.; Sha, D.; Yan, Y.; Liu, B.; Liao, X. Cascaded High Voltage Conversion Ratio Bidirectional Nonisolated DC–DC Converter With Variable Switching Frequency. *IEEE Trans. Power Electron.* **2017**, *33*, 1399–1409. [CrossRef]

79. Zhu, B.; Zeng, Q.; Vilathgamuwa, M.; Li, Y.; Chen, Y. A Generic Control-Oriented Model Order Reduction Approach for High Step-Up DC/DC Converters Based on Voltage Multiplier. *Energies* **2019**, *12*, 1971. [CrossRef]

80. Bhaskar, M.S.; Meraj, M.; Iqbal, A.; Padmanaban, S. Nonisolated Symmetrical Interleaved Multilevel Boost Converter with Reduction in Voltage Rating of Capacitors for High-Voltage Microgrid Applications. *IEEE Trans. Ind. Appl.* **2019**, *55*, 7410–7424. [CrossRef]

81. Bhaskar, M.S.; Almakhles, D.J.; Padmanaban, S.; Blaabjerg, F.; Subramaniam, U.; Ionel, D.M. Analysis and Investigation of Hybrid DC–DC Non-Isolated and Non-Inverting Nx Interleaved Multilevel Boost Converter (Nx-IMBC) for High Voltage Step-Up Applications: Hardware Implementation. *IEEE Access* **2020**, *8*, 87309–87328. [CrossRef]

82. Meraj, M.; Bhaskar, M.S.; Iqbal, A.; Al-Emadi, N.; Rahman, S. Interleaved Multilevel Boost Converter with Minimal Voltage Multiplier Components for High-Voltage Step-Up Applications. *IEEE Trans. Power Electron.* **2020**, *35*, 12816–12833. [CrossRef]

83. Zarepour, A.; Rajaei, A.; Mohammadi-Moghadam, H.; Shahparasti, M. A High Gain AC-DC Rectifier Based on Current-Fed Cockcroft-Walton Voltage Multiplier for Motor Drive Applications. *Sustainability* **2021**, *13*, 12317. [CrossRef]

84. Ramanathan, G.G.; Urasaki, N. Non-Isolated Interleaved Hybrid Boost Converter for Renewable Energy Applications. *Energies* **2022**, *15*, 610. [CrossRef]

85. Mayo-Maldonado, J.C.; Valdez-Resendiz, J.E.; Sanchez, V.M.; Rosas-Caro, J.C.; Claudio-Sanchez, A.; Puc, F.C. A novel PEMFC power conditioning system based on the interleaved high gain boost converter. *Int. J. Hydrog. Energy* **2018**, *44*, 12508–12514. [CrossRef]

86. Jang, Y.; Jovanovic, M.M. Interleaved Boost Converter with Intrinsic Voltage-Doubler Characteristic for Universal-Line PFC Front End. *IEEE Trans. Power Electron.* **2007**, *22*, 1394–1401. [CrossRef]

87. Shenoy, P.S.; Amaro, M.; Morroni, J.; Freeman, D. Comparison of a Buck Converter and a Series Capacitor Buck Converter for High-Frequency, High-Conversion-Ratio Voltage Regulators. *IEEE Trans. Power Electron.* **2016**, *31*, 7006–7015. [CrossRef]

88. Pradeep Shenoy, Design of a High-Frequency Series Capacitor Buck Converter, TI. Literature Number: SLUP337. 2016. Available online: https://www.ti.com/seclit/ml/slup337/slup337.pdf (accessed on 25 May 2022).

89. Rosas-Caro, J.C.; Escobar, G.; Valdez-Resendiz, J.E.; Maldonado, J.C.M.; Beltran-Carbajal, F.; Del-Valle-Soto, C. Analysis of the Input Current-Ripple in the Series-Capacitor Boost Converter. *IEEE Trans. Ind. Electron.* **2020**, *68*, 10303–10308. [CrossRef]

90. Ahmad, J.; Zaid, M.; Sarwar, A.; Lin, C.-H.; Ahmad, S.; Sharaf, M.; Zaindin, M.; Firdausi, M. A Voltage Multiplier Circuit Based Quadratic Boost Converter for Energy Storage Application. *Appl. Sci.* **2020**, *10*, 8254. [CrossRef]

91. Zaid, M.; Lin, C.-H.; Khan, S.; Ahmad, J.; Tariq, M.; Mahmood, A.; Sarwar, A.; Alamri, B.; Alahmadi, A. A Family of Transformer-less Quadratic Boost High Gain DC–DC Converters. *Energies* **2021**, *14*, 4372. [CrossRef]

92. Zheng, Y.; Xie, W.; Smedley, K.M. A Family of Interleaved High Step-Up Converters with Diode–Capacitor Technique. *IEEE J. Emerg. Sel. Top. Power Electron.* **2019**, *8*, 1560–1570. [CrossRef]

93. Truong, V.-A.; Luong, X.-T.; Nguyen, P.-T.; Quach, T.-H. The Improvement Switching Technique for High Step-Up DC–DC Boost Converter. *Electronics* **2020**, *9*, 981. [CrossRef]

94. Alzahrani, A.; Shamsi, P.; Ferdowsi, M. Interleaved Multistage Step-Up Topologies with Voltage Multiplier Cells. *Energies* **2020**, *13*, 5990. [CrossRef]

95. Park, S.; Park, Y.; Choi, S.; Choi, W.; Lee, K.-B. Soft-Switched Interleaved Boost Converters for High Step-Up and High-Power Applications. *IEEE Trans. Power Electron.* **2010**, *26*, 2906–2914. [CrossRef]

96. Kumar, P.; Veerachary, M. Z-Network Plus Switched-Capacitor Boost DC–DC Converter. *IEEE J. Emerg. Sel. Top. Power Electron.* **2019**, *9*, 791–803. [CrossRef]

97. Duong, T.-D.; Nguyen, M.-K.; Tran, T.-T.; Lim, Y.-C.; Choi, J.-H. Transformerless High Step-Up DC–DC Converters with Switched-Capacitor Network. *Electronics* **2019**, *8*, 1420. [CrossRef]

98. Axelrod, B.; Berkovich, Y.; Ioinovici, A. Switched-Capacitor/Switched-Inductor Structures for Getting Transformerless Hybrid DC–DC PWM Converters. *IEEE Trans. Circuits Syst. I Regul. Pap.* **2008**, *55*, 687–696. [CrossRef]

99. Axelrod, B.; Golan, G.; Berkovich, Y.; Shenkman, A. Diode–capacitor voltage multipliers combined with boost-converters: Topologies and characteristics. *IET Power Electron.* **2012**, *5*, 873–884. [CrossRef]

100. Vecchia, M.D.; Broeck, G.V.D.; Ravyts, S.; Driesen, J. Novel Step-Down DC–DC Converters Based on the Inductor–Diode and Inductor–Capacitor–Diode Structures in a Two-Stage Buck Converter. *Energies* **2019**, *12*, 1131. [CrossRef]

101. Malik, M.Z.; Tirth, V.; Ali, A.; Farooq, A.; Algahtani, A.; Verma, R.; Islam, S.; Irshad, K.; Abdalla, A.N. Efficient Topology for DC–DC Boost Converter Based on Charge Pump Capacitor for Renewable Energy System. *Int. J. Photoenergy* **2021**, *2021*, 6675720. [CrossRef]

102. Shen, M.; Peng, F.Z.; Tolbert, L.M. Multilevel DC–DC Power Conversion System with Multiple DC Sources. *IEEE Trans. Power Electron.* **2008**, *23*, 420–426. [CrossRef]

103. Sano, K.; Fujita, H. Voltage-Balancing Circuit Based on a Resonant Switched-Capacitor Converter for Multilevel Inverters. *IEEE Trans. Ind. Appl.* **2008**, *44*, 1768–1776. [CrossRef]

104. Chen, W.; Huang, A.Q.; Li, C.; Wang, G.; Gu, W. Analysis and Comparison of Medium Voltage High Power DC/DC Converters for Offshore Wind Energy Systems. *IEEE Trans. Power Electron.* **2012**, *28*, 2014–2023. [CrossRef]

105. Kawa, A.; Stala, R. SiC-Based Bidirectional Multilevel High-Voltage Gain Switched-Capacitor Resonant Converter with Improved Efficiency. *Energies* **2020**, *13*, 2445. [CrossRef]

106. Stillwell, A.; Pilawa-Podgurski, R.C.N. A Resonant Switched-Capacitor Converter with GaN Transistors for High-Efficiency Power Delivery to Series-Stacked Processors. *IEEE J. Emerg. Sel. Top. Power Electron.* **2019**, *8*, 3139–3150. [CrossRef]

107. Stala, R.; Waradzyn, Z.; Folmer, S. DC–DC High-Voltage-Gain Converters with Low Count of Switches and Common Ground. *Energies* **2020**, *13*, 5657. [CrossRef]

108. Xu, J.; Gu, L.; Rivas-Davila, J. Effect of Class 2 Ceramic Capacitor Variations on Switched-Capacitor and Resonant Switched-Capacitor Converters. *IEEE J. Emerg. Sel. Top. Power Electron.* **2019**, *8*, 2268–2275. [CrossRef]

109. Law, K.; Cheng, K.; Yeung, Y. Design and analysis of switched-capacitor-based step-up resonant converters. *IEEE Trans. Circuits Syst. I: Regul. Pap.* **2005**, *52*, 943–948. [CrossRef]

110. Cao, D.; Peng, F.Z. Multiphase Multilevel Modular DC–DC Converter for High-Current High-Gain TEG Application. *IEEE Trans. Ind. Appl.* **2011**, *47*, 1400–1408. [CrossRef]
111. Cao, D.; Peng, F.Z. Zero-Current-Switching Multilevel Modular Switched-Capacitor DC–DC Converter. *IEEE Trans. Ind. Appl.* **2010**, *46*, 2536–2544. [CrossRef]
112. Zou, K.; Scott, M.J.; Wang, J. Switched-Capacitor-Cell-Based Voltage Multipliers and DC–AC Inverters. *IEEE Trans. Ind. Appl.* **2012**, *48*, 1598–1609. [CrossRef]
113. Valdez-Reséndiz, J.; Claudio-Sánchez, A.; Rosas-Caro, J.; Guerrero-Ramírez, G.; Mayo-Maldonado, J.; Tapia-Hernández, A. Resonant switched capacitor voltage multiplier with interleaving capability. *Electr. Power Syst. Res.* **2016**, *133*, 365–372. [CrossRef]
114. Uno, M.; Nakane, T.; Shinohara, T. LLC Resonant Voltage Multiplier-Based Differential Power Processing Converter Using Voltage Divider with Reduced Voltage Stress for Series-Connected Photovoltaic Panels under Partial Shading. *Electronics* **2019**, *8*, 1193. [CrossRef]
115. Lei, H.; Hao, R.; You, X.; Li, F. Nonisolated High Step-Up Soft-Switching DC–DC Converter with Interleaving and Dickson Switched-Capacitor Techniques. *IEEE J. Emerg. Sel. Top. Power Electron.* **2019**, *8*, 2007–2021. [CrossRef]
116. Stala, R.; Waradzyn, Z.; Folmer, S. Input Current Ripple Reduction in a Step-Up DC–DC Switched-Capacitor Switched-Inductor Converter. *IEEE Access* **2022**, *10*, 19890–19904. [CrossRef]
117. Górecki, P. Electrothermal Averaged Model of a Diode–IGBT Switch for a Fast Analysis of DC–DC Converters. *IEEE Trans. Power Electron.* **2022**, *37*, 13003–13013. [CrossRef]
118. Górecki, P.; Górecki, K. Methods of Fast Analysis of DC–DC Converters—A Review. *Electronics* **2021**, *10*, 2920. [CrossRef]